Accepted Manuscript

Discovery of novel human inosine 5′-monophosphate dehydrogenase 2 (*h*IMPDH2) inhibitors as potential anticancer agents

Chetan P. Shah, Prashant S. Kharkar

PII: S0223-5234(18)30788-8

DOI: 10.1016/j.ejmech.2018.09.016

Reference: EJMECH 10727

To appear in: *European Journal of Medicinal Chemistry*

Received Date: 12 May 2018

Revised Date: 13 August 2018

Accepted Date: 5 September 2018

Please cite this article as: C.P. Shah, P.S. Kharkar, Discovery of novel human inosine 5′-monophosphate dehydrogenase 2 (*h*IMPDH2) inhibitors as potential anticancer agents, *European Journal of Medicinal Chemistry* (2018), doi: 10.1016/j.ejmech.2018.09.016.

Graphical abstract

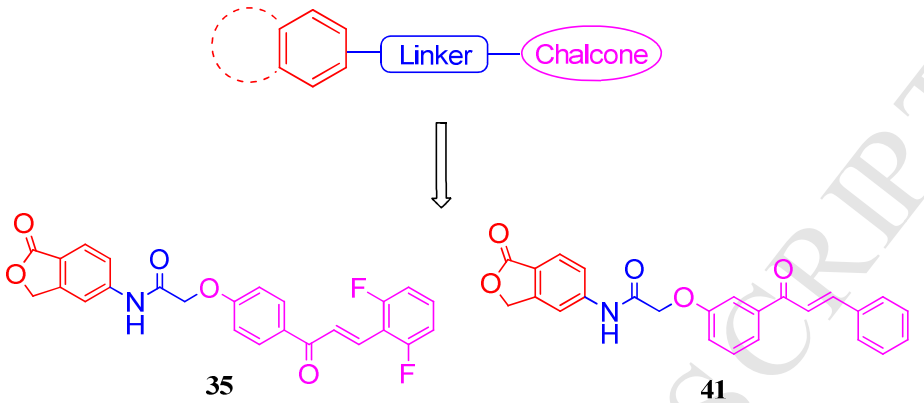

*h*IMPDH2 inhibition **94.15 %** @ 10 µM
IC_{50}: **0.36** µM

*h*IMPDH2 inhibition **93.68 %** @ 10 µM
IC_{50}: **0.43** µM

Better cellular potency than MPA

Discovery of novel human inosine 5′-monophosphate dehydrogenase 2 (*h*IMPDH2) inhibitors as potential anticancer agents

Chetan P. Shah and Prashant S. Kharkar*

Department of Pharmaceutical Chemistry, Shobhaben Pratapbhai Patel School of Pharmacy and Technology Management, SVKM's NMIMS, V. L. Mehta Road, Vile Parle (West), Mumbai 400 056. India.

* Corresponding Author:
Prashant S. Kharkar, PhD
E-mail: Prashant.kharkar@nmims.edu

Abstract

The enzyme inosine 5'-monophosphate dehydrogenase (IMPDH) catalyzes an essential step in the *de novo* biosynthesis of guanine nucleotides, and thus regulates the guanine nucleotide pool required for cell proliferation. Of the two isoforms, human IMPDH type 2 (*h*IMPDH2) is a validated molecular target for potential immunosuppressive, antiviral and anticancer chemotherapy. In search of newer *h*IMPDH2 inhibitors as potential anticancer agents, three novel series (**A**: 5-aminoisobenzofuran-1(3*H*)-one, **B**: 3,4-dimethoxyaniline and **C**: benzo[*d*]-[1,3]dioxol-5-ylmethanamine) were synthesized and evaluated for in vitro and cell-based activities. A total of 37 molecules (**29-65**) were screened for their in vitro *h*IMPDH2 inhibition, with particular emphasis on establishing their structure–activity relationship (SAR) trends. Eight compounds (hits, **30**, **31**, **33-35, 37**, **41** and **43)** demonstrated significant enzyme inhibition (>70% @ 10 µM); especially the A series molecules were more potent than B series (<70% inhibition @ 10 µM), while C series members were found to be inactive. The *h*IMPDH2 IC_{50} values for the hits ranged from 0.36 to 7.38 µM. The hits displaying >80% *h*IMPDH2 inhibition (**30**, **33**, **35**, **41** and **43**) were further assessed for their cytotoxic activity against cancer cell lines such as MDA-MB-231 (breast adenocarcinoma), DU145 (prostate carcinoma), U87 MG (glioblastoma astrocytoma) and a normal cell line, NIH-3T3 (mouse embryonic fibroblast) cell lines using MTT assay. Most of the compounds exhibited higher cellular potency against cancer cell lines and notably lower toxicity towards NIH-3T3 cells compared to mycophenolic acid (MPA), a prototypical *h*IMPDH2 inhibitor. Two of the series A hits (**30** and **35**) were evaluated in human peripheral blood mononuclear cells (hPBMC) assay and found to be better tolerated than MPA. The calculated/predicted molecular and physicochemical properties were satisfactory with reference to drug-likeness. The molecular docking studies clearly demonstrated crucial interactions of the hits with the cofactor-binding site of *h*IMPDH2, further providing critical information for refining the design strategy. The present study reports the design and discovery of structurally novel *h*IMPDH2 inhibitors as potential anticancer agents and provides a guide for further research on the development of safe and effective anticancer agents, especially against glioblastoma.

Keywords: IMPDH; *h*IMPDH2 inhibitors; 5-aminoisobenzofuran-1(3*H*)-one; MTT assay; anticancer agents

1. Introduction

Cancer is a swiftly growing disease of the current era and represents one of the biggest healthcare issues for the human race. It is the leading cause of death irrespective of the developments in the disease diagnosis, treatment and prevention methods [1–3]. Cancer is characterized by uncontrolled growth and spread of abnormal cells due to their high metabolic state, i.e., increased cellular metabolism. Enzymes that are critical for cell viability and that exhibit markedly different activities or expression levels in the disease state tissues are especially promising molecular targets for cancer therapeutics [4]. It is a genetic disease (genetic instabilities) that progresses via development of multistep carcinogenesis with participation from various cell signalling pathways and apoptosis, and as a result, cancer is extremely intricate to fight [5]. Mostly, cancer begins as a local disease, but it metastasizes over time in most cases, making it difficult to cure. These cells construct hostile microenvironment and are not only adapted to this reserve environment but also, grow and migrate to distant tissues [6]. Mutations in DNA repair genes (*p21, p22, p27, p51* and tool box for DNA), tumor suppressor genes (*p53, NF1, NF2, RB* and biological breaks), oncogenes [*myc, raf, bcl-2, ras* (biological accelerators)] and genes involved in cell growth metabolism are thought to be responsible for the uncontrolled proliferation of normal cells which are transformed into malignant cells [7].

Despite the availability of several anticancer drugs, it is a challenging job for a medicinal chemist to design newer agents that target tumor-specific pathways due to complicated problems like tumor heterogeneity, frequent oncogenic mutations, multidrug resistance (MDR), less therapeutic efficacy, debilitating adverse effects and poor bioavailability issues. This necessitates the development of safer and targeted anticancer agents [8,9]. Rapid proliferation is an important characteristic of cancer cells. This ultimately requires, in addition to other factors, an expansion of the guanine nucleotide pool that generally cannot be sustained by salvage pathways. This is where the importance of inosine 5'-monophosphate dehydrogenase (IMPDH, an enzyme linked with proliferation and malignancy) comes in picture. The enzyme IMPDH (EC 1.1.1.205) catalyzes a rate-limiting step in the *de novo* synthesis of guanine nucleotides which are essential for cell proliferation, cell signalling, and as an energy source [10–12].

The enzyme IMPDH catalyzes the oxidation of inosine 5'-monophosphate (IMP) to xanthosine 5'-monophosphate (XMP), which is then converted into guanosine 5'-monophosphate (GMP) by GMP synthase. IMP also serves as a substrate for the biosynthesis

of adenosine 5'-monophosphate (AMP). Consequently, inhibition of IMPDH causes a variety of biological responses, such as reduction in the guanine nucleotide pools resulting in cell proliferation arrest (interruption of DNA and RNA syntheses) [13], a decline in intracellular signalling (G-protein-mediated signal transduction) [14–16], down-regulation of *c-myc* and *K-ras* oncogenes in vitro [17]. Also, IMPDH inhibition is associated with an up-regulation of *p53* (commonly mutated protein in human cancers) [18], *p21*, *bax* and a down-regulation of *bcl-2*, survivin and *p27* protein [19]. These observations pose IMPDH as an attractive target to suppress tumor cell growth.

Human IMPDH enzyme exists in two isoforms - *h*IMPDH1 and *h*IMPDH2 with high sequence similarity (84%) and similar kinetic properties. The *h*IMPDH1, expressed at relatively constant levels in both normal and neoplastic cells, seems to play a general housekeeping role while the expression of *h*IMPDH2 is up-regulated in human neoplastic cells [20]. The disproportionate increase in *h*IMPDH2 activity in neoplastic cells has made it a significant target for the development of anticancer drug discovery [4,21]. Also, *h*IMPDH2 has historically been a major drug target for immunosuppressive [22,23], antiviral [24] and antimicrobial chemotherapy [10,25]. Mycophenolic acid (MPA) (**A**, Figure 1), a natural product, is a reversible, potent and uncompetitive inhibitor of IMPDH and is a known anticancer and immunosuppressive agent. Mycophenolate mofetil, a prodrug of MPA (MMF, **B**, Figure 1), has been approved for the treatment of acute allograft rejection following kidney transplant. The MPA and its related forms MMF or MPA sodium (**C**, Figure 1) (MPS) cause dose-limiting gastrointestinal (GI) toxicities. However, adverse effects related to the treatment with MPA-based drugs, such as diarrhea, leukopenia, sepsis and vomiting, are the barriers to the administration of higher doses and thereby more effective treatment [26]. Similarly, the nucleoside analogs which are competitive IMPDH inhibitors, e.g., tiazofurin (**D**), ribavirin (**E**) and mizoribine (**F**) (Figure 1) (bioprecursors which need intracellular activation by phosphorylation) have unfavourable tolerability profiles too. Thus, there is an urgent need for newer, safer, potent and orally bioavailable *h*IMPDH2 inhibitors with a broad spectrum of anticancer activity [27,28].

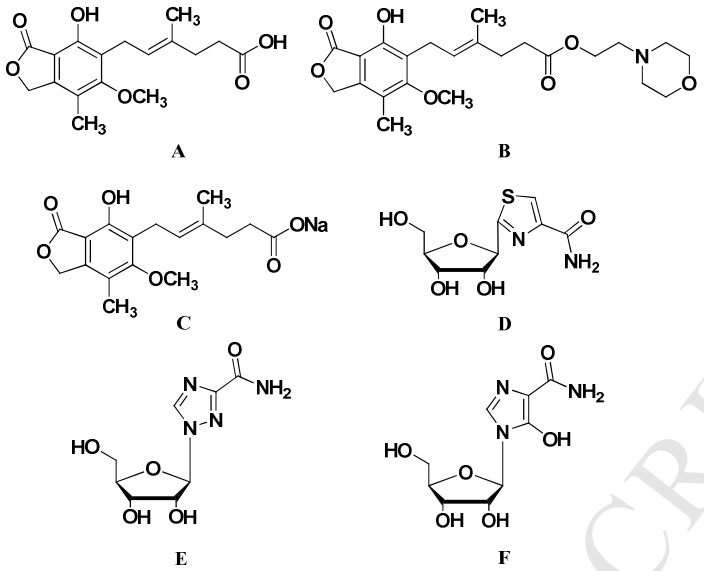

Figure 1. Clinically used IMPDH inhibitor drugs

In order to develop potent IMPDH inhibitors, significant efforts were focused on various structural modifications of MPA using bio-isosteric replacements and innumerable structural derivatives with different scaffolds but with limited success [4,29]. MPA has been demonstrated to be an effective inducer of differentiation in a number of cancer cell lines and displayed synergism with imatinib in the treatment of chronic myologenous leukemia (CML) [30]. Furthermore, antitumor activities of several MPA derivatives are reported [31–35]. These outcomes strongly support the role of MPA as a potential anticancer drug. Moreover, MPA, being an acid, is likely to be prevented from entering in the CNS. There are no reports in the literature citing this fact that MPA could be useful for treating gliomas, dreadful cancers of the CNS [36]. Earlier reports proposed that diminutive structural alteration of MPA was damaging to its IMPDH inhibitory activity. Therefore, it was crucial to select the design strategy leading to retention of the inhibitory potential against *h*IMPDH2. Also, it was reported that the isobenzofuran-1(3*H*)-one part and the *trans* configuration of MPA were important to retain the inhibitory potential against *h*IMPDH2 [12,37–44]. Working on similar thought process, in this report, we have outlined the design, synthesis and biological evaluation of three novel series of potential *h*IMPDH2 inhibitors (**A**, **B** and **C**, Figure 2). The title compounds were evaluated for in vitro *h*IMPDH2 inhibition and further assessed for their cellular potency against MDA-MB-231 (breast adenocarcinoma), DU145 (prostate carcinoma), U87 MG (glioblastoma astrocytoma) and NIH-3T3 (mouse embryonic fibroblast) cell lines. In addition, their structure–activity relationships (SAR) trends were studied carefully throughout in order to guide further improvements in potency and other

physicochemical properties. The results of the present study provide insights into the design and development of novel *h*IMPDH2 inhibitors as potential anticancer agents.

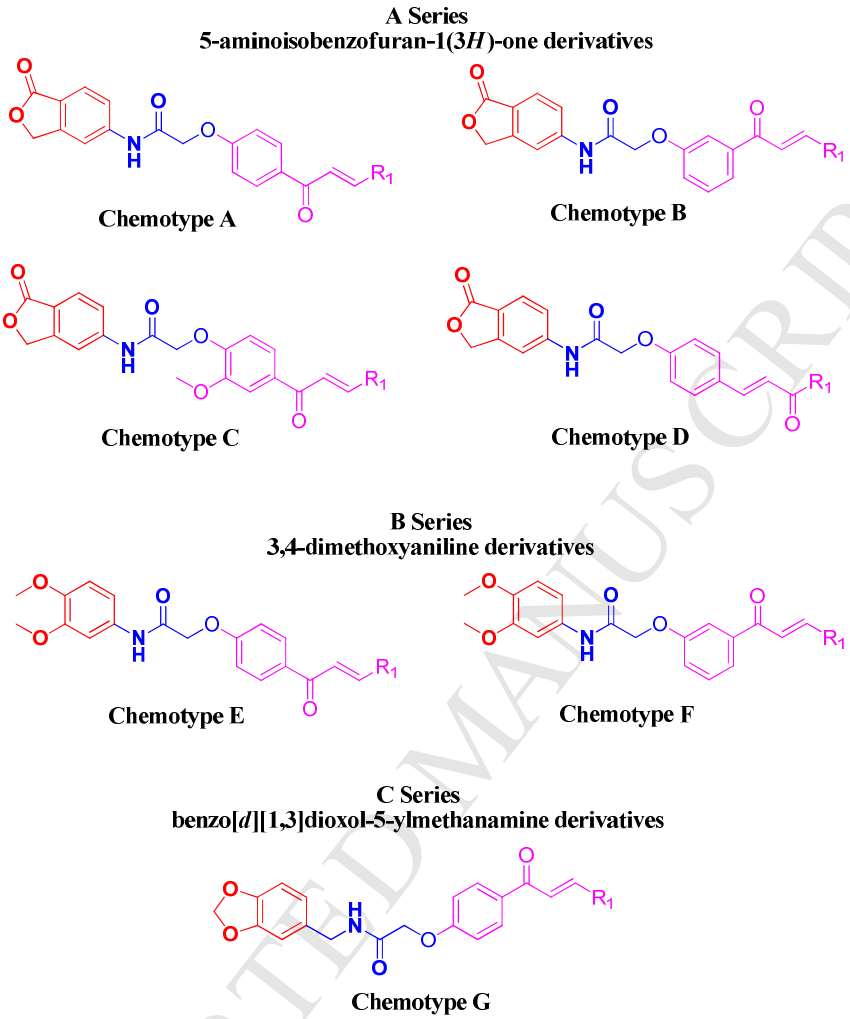

Figure 2. Representative chemotypes (**A-G**) of novel *h*IMPDH2 inhibitors reported in this study

2. Results and discussion

Mycophenolic acid is a well-known *h*IMPDH2 inhibitor with several pharmacological activities [12]. Its antitumor activity decreased or completely lost when any structural modification, not matter how subtle, was done [31,32]. Numerous classes of compounds such as amides, oxazolyl indoles, phenylamino oxazoles, amino-oxazoles, guanidines, triazines, isoquinolines, quinolones, quinazolinones, quinazolinethiones and quinazolinediones, indoles and acridones have been synthesized using molecular modification approach [45]. Unfortunately, none of these molecules occurred to be advantageous as anticancer compounds.

Mycophenolic acid exhibits unfavourable metabolism (7-O-glucuronide, major metabolite; acyl glucuronide, minor metabolite) which is responsible for its higher dose, dosing frequency, GI side effects and variable exposure. The phenolic –OH on the iso-benzofuranone substructure is the main culprit. It would be worthwhile to come up with molecules with retained or improved potency but devoid of the issues with MPA. With this thing in mind, in the present study, we attempted to discover potent and novel *h*IMPDH2 inhibitors. The increasing knowledgebase of the IMPDH structure laid foundation for summarizing essential chemical features, which may inspire the development of novel IMPDH inhibitors and their spatial alignment. Three substructures namely, 5-aminoisobenzofuran-1(3*H*)-one **(23)**, 3,4-dimethoxyaniline **(24)**, benzo[*d*][1,3]dioxol-5-ylmetha- namine **(25)** linked with substituted chalcones, were used as cores. These scaffolds were selected to mimic the isobenzofuran-1(3*H*)-one part and the *trans* configuration of the MPA.

2.1. Chemistry

The derivatives **29-65** (Series A-C) were synthesized as outlined (Schemes 1-3). The general synthetic route to target chalcones (General procedure A, **1-22**) is depicted in Scheme 1. All the chalcones were synthesized by Claisen-Schmidt condensation using substituted acetophenones and (hetero)aryl aldehydes in presence of NaOH as base in EtOH as reported earlier [46]. The chloroacetamides scaffolds (General procedure B, **26-28**) were synthesized using the starting amines (**23-25**) and chloroacetyl chloride in dry THF in the presence of TEA at 0 °C (Scheme 2). This was followed by O-arylation reaction using K_2CO_3/DMF to yield the title compounds (General procedure C) **29-65** (Scheme 3, Table 1) [47].

Scheme 1[a]. General scheme for synthesis of substituted chalcones **(1-22)**

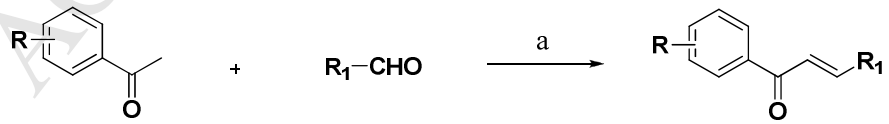

Substituted acetophenone **Substituted aldehyde** **Chalcones (1-22)**

[a]Reagents and conditions: a. 20% NaOH, EtOH, 5 °C to RT, 24-72 hr

2.2. Biological activity

2.2.1. In vitro *h*IMPDH2 inhibition assay

All 37 molecules were screened in-house for in vitro *h*IMPDH2 inhibition at 10 µM concentration. The results are shown in Table 1 and Figure 1S (see *Supplementary Information* section). Compounds **30**, **31**, **33-35**, **37**, **41** and **43** (hits) exhibited >70% inhibition. The hits were further taken up for IC_{50} determination. Overall, series A molecules (**29-50**) were more active than their series B counterparts (**51-60**), while molecules from C series (**61-65**) were inactive at the concentration tested (Table 1). These observations unequivocally highlighted the significance of isobenzofuran-1(3*H*)-one substructure from MPA for mediating crucial interactions with enzyme residues for potent inhibition of *h*IMPDH2.

Series A: The molecules were further divided in four chemotypes, A to D (Figure 2) for easy interpretation of the SAR trends. There was gradual increase in % inhibition in case of chemotype A when the size of R_1 increased from phenyl (**37**, 79%, Table 1) to 3′-OMePh (**33**, 91%). Shifting the 3′–OMe substituent to 4′-position increased the activity slightly (**30**, 96%), demonstrating the critical role of the H-bond acceptor functionality at the distal end of the molecule. Increasing the size of the 4′-substituent from –OMe to –OEt (**48**, 65%), O-Pr^n (**49**, 60%), –O-Bu^n (**50**, 58%) resulted in systematic decrease in % inhibition. Additional increase in bulk led to substantial reduction in the inhibitory activity featuring limited space available in the binding site of the enzyme (**45-47**, 37-52%). Further increasing the size of R_1 by placing one or more additional substituent(s) on the Ph ring decreased the activity (**29**: 65%; **34**:71%). Placing the electron-withdrawing substituents on the Ph ring such as 2′-Cl (**32**, 60%), 4′-Cl (**44**, 62%), 4′-NO_2 (**36**, 63%) led to reduction in activity over their unsubstituted counterpart. Compound **35** with R_1 = 2′,6′-diFPh substituent exhibited increased % inhibition (94%). This may be due to smaller size of F and its H-bonding potential leading to significant increase in binding energy with increase in % inhibition.

Scheme 2[a]. General scheme for synthesis of substituted chloroacetamides **(26-28)**

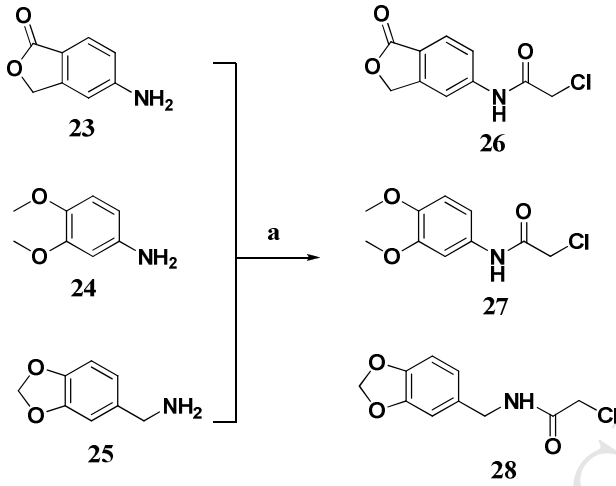

[a]Reagents and conditions: a. Chloroacetyl chloride, TEA, THF, 0 °C to RT, overnight

Scheme 3[a]. General scheme for synthesis of final compounds **(29-65)**

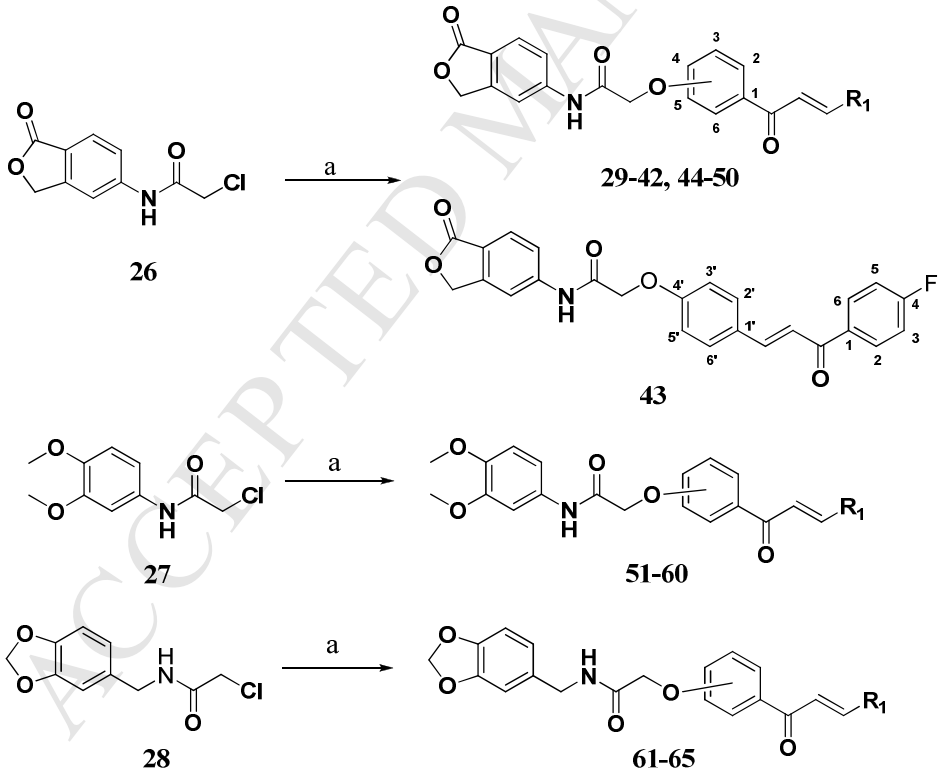

[a]Reagents and conditions: a. **1-22**, DMF, K_2CO_3, RT, 16 hr

Substitution by the heteroaryl rings – 2′-thienyl (**31**, 76%) and 2′-furyl (**38**, 57%) – clearly resulted in reduced activity. It is well-known that thiophene is very similar to benzene

with respect to its aromatic character, while furan is the least aromatic and way different from benzene. This was worth noting that sufficient aromatic π cloud was required for higher activity. There may be underlying π-π stacking interactions with the enzyme residues.

For chemotypes B and C, similar SAR trends as above were seen. Compound **41** (94%, Table 1) was more active than its chemotype A counterpart (**37**), further hinting us about the narrow cavity at the distal end of the molecule. Increased steric bulk in the form of additional substituents on the aromatic ring led to more or less reduced % inhibition (**39**, **40** and **42**). Compound **43** (chemotype D, Figure 2, Table 1) with reversed 'enone' functionality exhibited slight reduction in potency (88%). Overall, the series A molecules exhibited prominent SAR trends which would be helpful in future design strategies.

Series B*:* The proximal part of the molecule contained a 3,4-dimethoxyphenyl substructure in this set of molecules. This single change led to drastic reduction in the % inhibition over their series A counterparts (**51** versus **30** – three-fold reduction in activity, Table 1), (**52** versus **33** – three-fold reduction in activity) irrespective of the Chemotypes - E and F, except compound **55** which retained the activity (**55** versus **48**). This reiterated the crucial role played by the nature of the proximal part, which is likely to interfere with IMP stacking during the binding process.

Series C: All the molecules from this series with 3,4-methylenedioxy substructure as the proximal part, were inactive. They completely failed to demonstrate any inhibition at the concentrations tested. In summary, we have successfully identified a novel series of molecules with appreciable *h*IMPDH2 inhibition. The insights gained from the initial data could potentially drive the design and development of potent inhibitors.

Overall, among three series (A-C), all the identified promising hits were from series A indicating the importance of 5-aminoisobenzofuran-1(3*H*)-one substructure for stacking with IMP at the proximal end of the molecule and might be interacting with the active site residues (Gly 326 and Thr 333) similar to MPA. While the other two series B (3,4-dimethoxyaniline) and series C (benzo[*d*]-[1,3]dioxol-5-ylmethanamine) possibly lacked these interactions and hence were less active or inactive.

The hit molecules - **30**, **31**, **33-35, 37**, **41** and **43** - all from series A, with >70% inhibition at 10 μM were used for IC_{50} determination, along with MPA, the positive control. The IC_{50} values of the hits (0.36 to 7.38 μM) were comparable to MPA (0.25 μM). Compounds **31**, **34** and **37** with <80% enzyme inhibition were not persuaded further for cell-based assays; rest of the hits were.

Table 1. Structural features and *h*IMPDH2 % inhibition of derivatives **29-65** at 10 μM

Compound	Chemotype	R_1	*h*IMPDH2	
			% Inhibition[a]	IC_{50} (μM)[b]
MPA	-	-	99.90 ± 1.20	0.25 ± 0.03
29	A	3′,4′-dimethoxyphenyl	65.45 ± 3.56	n.d.[c]
30	A	4′-methoxyphenyl	95.63 ± 4.36	0.66 ± 0.38
31	A	2′-thienyl	76.30 ± 2.12	4.54 ± 1.70
32	A	2′-chlorophenyl	59.52 ± 2.11	n.d.[c]
33	A	3′-methoxyphenyl	91.45 ± 1.67	0.36 ± 0.04
34	A	3′,4′,5′-trimethoxyphenyl	71.35 ± 1.75	7.38 ± 0.74
35	A	2′,6′-difluorophenyl	94.15 ± 3.22	0.36 ± 0.12
36	A	4′-nitrophenyl	63.18 ± 1.49	n.d.[c]
37	A	Phenyl	79.08 ± 4.83	0.79 ± 0.25
38	A	2′-furyl	57.31 ± 3.92	n.d.[c]
39	B	3′,4′-dimethoxyphenyl	56.97 ± 2.33	n.d.[c]
40	B	3′,4′,5′-trimethoxyphenyl	63.66 ± 1.39	n.d.[c]
41	B	Phenyl	93.68 ± 1.67	0.43 ± 0.04
42	C	3′,4′,5′-trimethoxyphenyl	19.88 ± 3.07	n.d.[c]
43	D	4-fluorophenyl	87.86 ± 1.22	0.57 ± 0.03
44	A	4′-chlorophenyl	62.15 ± 2.56	n.d.[c]
45	A	4′-benzyloxyphenyl	52.23 ± 1.85	n.d.[c]
46	A	4′-(2,4-dichlorobenzyloxy)phenyl	36.67 ± 2.42	n.d.[c]
47	A	4′-(4-chlorobenzyloxy)phenyl	39.12 ± 0.93	n.d.[c]
48	A	4′-ethoxyphenyl	65.45 ± 1.45	n.d.[c]
49	A	4′-propoxyphenyl	60.14 ± 1.74	n.d.[c]
50	A	4′-butoxyphenyl	57.68 ± 3.27	n.d.[c]
51	E	4′-methoxyphenyl	33.56 ± 2.85	n.d.[c]
52	E	3′-methoxyphenyl	28.84 ± 1.31	n.d.[c]
53	F	3′,4′-dimethoxyphenyl	23.29 ± 1.48	n.d.[c]
54	E	3′,4′,5′-trimethoxyphenyl	20.61 ± 3.16	n.d.[c]
55	E	4′-ethoxyphenyl	63.50 ± 1.79	n.d.[c]
56	E	2′-chlorophenyl	25.67 ± 2.53	n.d.[c]
57	E	4′-chlorophenyl	30.12 ± 1.28	n.d.[c]

58	E	2′,6′-difluorophenyl	35.93 ± 2.16	n.d.[c]
59	E	2′-furyl	21.34 ± 1.61	n.d.[c]
60	E	2′-thienyl	24.52 ± 1.99	n.d.[c]
61	G	4′-methoxyphenyl	n.a.[d]	n.d.[c]
62	G	3′,4′-dimethoxyphenyl	n.a.[d]	n.d.[c]
63	G	3′,4′,5′-trimethoxyphenyl	n.a.[d]	n.d.[c]
64	G	4′-ethoxyphenyl	n.a.[d]	n.d.[c]
65	G	2′,6′-fluorophenyl	n.a.[d]	n.d.[c]

[a] All the data are expressed as ± SD (results are average of duplicate analysis)
[b] All the data are expressed as ± SD (results are average of triplicate analysis). IC_{50} value was determined when the inhibitory rate of compound is higher than 70% at the concentration of 10 µM.
[c] n.d. = not determined; [d] n.a. = not active

2.2.2. Cell viability assay

Cytotoxic activity of hits **30**, **33**, **35**, **41** and **43** (>80% *h*IMPDH2 inhibition at 10 µM) and MPA was evaluated against cell lines: MDA-MB-231 (breast adenocarcinoma), DU145 (prostate carcinoma), U87 MG (glioblastoma astrocytoma) and NIH-3T3 (mouse embryonic fibroblast cells) using colorimetric MTT assay. The results are reported in Table 2 and Figure 2S (see *Supplementary Information* section). The IC_{50} values were expressed in µM. Cisplatin and doxorubicin HCl were used as positive controls in addition to MPA. Most of the hits exhibited better activity than MPA in this assay. It might be difficult for MPA, an acid, to cross the cell membrane and exhibit activity. In fact, the lowest potency for MPA was found against U87 MG, a glioblastoma cell line. In contrast, the hits were more lipophilic (average AlogP 3.98). Out of the five hits tested against different cell lines, **41** exhibited greater potency compared to others against MDA-MB-231 and DU145 cell lines. Compound **41** was ~4-fold (MDA-MB-231) and 1.7-fold (DU145) more potent than MPA, respectively. Compound **35** showed promising activity against U87 MG (~3-fold more potent than MPA) (Table 2).

For any new chemical entity (NCE) to become a successful drug, it is not only effective against the diseased cells but also does minimum harm to the normal cells. The hits (**30**, **33**, **35**, **41** and **43**) were evaluated against NIH-3T3 cell line (normal cell line) to determine their selectivity. The hits were found to be relatively less toxic compared to MPA and cisplatin and doxorubicin (standard chemotherapeutic drugs) and no significant cytotoxicity was observed even at higher concentration (100 µM) (Figure 3 and Table 1S, *Supplementary Information* section). Also, hits (**30**, **35**) and MPA were tested in hPBMC

proliferation assay (see *Supplementary Information* section for protocol). The % cell viability was found to be 63% for MPA, 86% for **30** and 77% for **35** which clearly demonstrated that **30** and **35** were less toxic to hPBMCs in comparison to MPA. The possibility of the title compounds exhibiting higher activity than MPA could be due to their ability to penetrate the cells owing to higher AlogP values. The higher cellular potency of these derivatives over MPA was definitely a headway in the direction of the goal, i.e., to discover a novel *h*IMPDH2 inhibitor as potential anticancer agent.

Table 2. Cytotoxicity data of the hits in MTT assay

Sr. No.	Compound	IC_{50} (μM) ± SD[a]		
		MDA-MB-231[b]	DU145[c]	U87 MG[d]
1	**Cisplatin**	50.40 ± 1.10	34.47 ± 0.78	21.32 ± 0.39
2	**Doxorubicin HCl**	0.54 ± 0.08	0.21 ± 0.06	0.11 ± 0.02
3	**MPA**	4.38 ± 0.06	2.94 ± 0.09	10.69 ± 0.21
4	**30**	3.03 ± 0.27	2.13 ± 0.18	4.90 ± 0.18
5	**33**	3.42 ± 0.19	2.55 ± 0.28	5.75 ± 0.24
6	**35**	2.41 ± 0.10	1.90 ± 0.15	**3.67 ± 0.14**
7	**41**	**1.10 ± 0.09**	**1.75 ± 0.08**	3.97 ± 0.12
8	**43**	5.42 ± 0.14	6.88 ± 0.13	6.05 ± 0.24

[a]All the data are expressed as ± SD (results are average of triplicate analysis). [b]MDA-MB-231 (breast adenocarcinoma); [c]DU145 (prostate carcinoma); [d]U87 MG (glioblastoma astrocytoma).

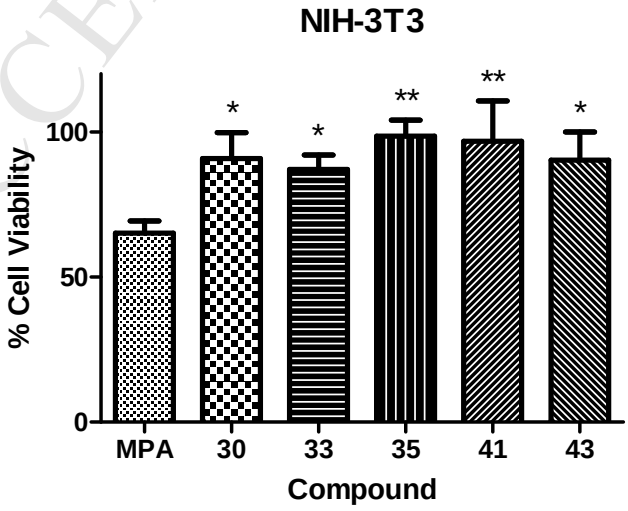

Figure 3. % Cell viability of the compounds against NIH-3T3 cell line (data are mean ± SD,

n=3) (Asterisk above columns indicate statistically significant difference compared to MPA. * = p< 0.05, ** = p< 0.01, *** = p< 0.001)

2.3 Computational studies

2.3.1. *In silico* physicochemical property prediction

The molecular properties play crucial role in the random-walk and the drug-receptor interactions. At the design stage, we ensured that the compounds passed all the drug-like filters (data not shown). Although the presence of aromatic $–NO_2$, -Cl, as well as heterocycles like thiophene and furan are a strict no-no in molecule structures, we still synthesized these molecules as a part of SAR investigations. The interesting results from the in vitro enzyme inhibition and cell-based assays compelled us to investigate the physicochemical property profiles of the synthesized compounds in detail. The initial part of the study dealt with the molecular properties calculation/prediction using Canvas module of Schrödinger Small-Molecule Drug Discovery Suite [49]. The detailed analysis of the property profiles of all the compounds (data not shown) led to interesting outcome. It was observed that the limited size at the distal end of the molecule supposedly contributed to increased *h*IMPDH2 activity. A bubble plot of these properties is shown for clear understanding (Figure 4).

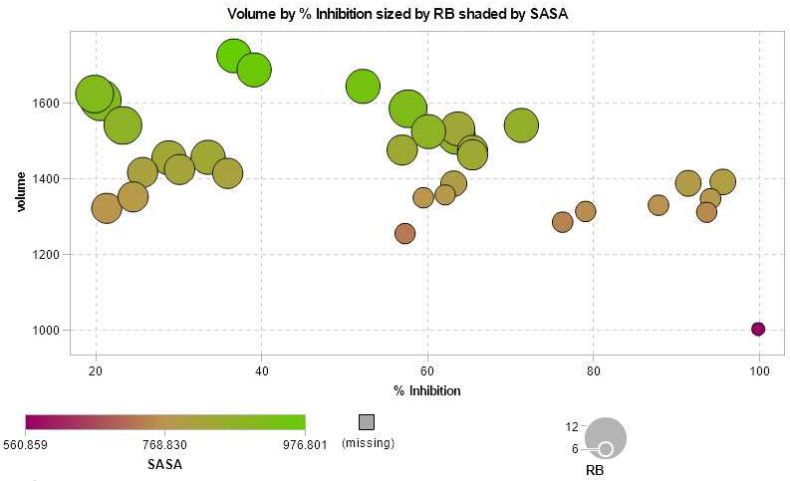

Figure 4. Bubble plot of volume by % inhibition sized by RB shaded by SASA

We further calculated/predicted molecular and physicochemical parameters of the hits (**30**, **33**, **35**, **41** and **43**) and MPA using QikProp module of Schrödinger Small-Molecule Drug Discovery Suite [49]. The results are shown in Table 3. The AlogP values of the hits were in the range 3.81 to 4.24 (**MPA** AlogP: 3.11). All the hits passed Lipinski's rule of five filter. The properties related to membrane permeability such as QPPCaco and QPPMDCK as well as % human oral absorption were better than MPA and found satisfactory. In summary,

the molecular/ physicochemical properties calculation/prediction confirmed the drug-likeness and acceptable pharmacokinetic parameters of the hits.

The present study finally culminated in a set of newer, relatively potent *h*IMPDH2 inhibitors which have shown higher anticancer activity in vitro. The hits are likely to exhibit acceptable pharmacokinetic profiles and in vivo activity, as predicted from the *in silico* studies. Further work in this direction will yield novel and potent *h*IMPDH2 inhibitors ready to enter further development stages.

Table 3. Predicted physicochemical properties

Sr. No.	Property	Compound					
		MPA	**30**	**33**	**35**	**41**	**43**
1	**MW**	320.34	443.45	443.45	449.4	413.42	431.41
2	**AlogP**	3.11	3.81	3.81	4.24	3.82	4.03
3	**PSA**	117.29	122.79	122.80	114.66	114.63	114.60
4	**QPlogS**	-3.41	-5.87	-5.77	-6.27	-5.54	-5.99
5	**QPlogPo/w**	2.5	3.50	3.49	3.83	3.40	3.65
6	**QPPCaco**	36.63	238.26	245.62	246.69	245.5	245.77
7	**QPlogBB**	-1.59	-1.97	-1.93	-1.68	-1.82	-1.74
8	**QPPMDCK**	17.64	104.96	108.47	284.63	108.41	195.9
9	**% Human Oral Absorption**	69.57	89.98	90.16	92.19	89.64	91.09

2.3.2. Molecular docking

To identify the potential structural features of the ligand and its interaction with the cofactor-binding site of *h*IMPDH2, molecular docking studies were performed. The results of these studies i.e., docking scores and interaction energy of the ligands with the *h*IMPDH2 residues are listed in Table 4. Further, the docked poses of **MPA** and two most potent hits (**35** and **41**) are shown in Figure 5. It is clear observed that **MPA**, **35** and **41** nicely occupied the *hIMPDH2* cofactor-binding site lined by Asp274, Ser276, Gly326, Thr333 and Gln441. The 2-oxo group of the isobenzofuran-1-(3*H*)-one of **MPA**, **35** and **41** formed strong H-bond with side-chain -OH of Thr333; **35** exhibited additional H-bond with backbone -NH of Gly326. MPA -COOH group formed a strong H-bond with side-chain -OH of Ser276. The hit **41**

demonstrated similar interaction involving distal chalcone -C=O group. The aromatic -NH of **35** formed a H-bond with -COO^- of Asp274. The chalcone portion of the hits was found in a region surrounded by several hydrophobic residues. Overall, the binding modes of **41** and **35** clearly revealed additional interactions of the hits with the residues lining the cofactor-binding pocket of *h*IMPDH2. These studies clearly demonstrated that isobenzofuran-1-(3*H*)-one substructure was responsible for efficient binding (i.e., anchoring) of the hits in the cofactor-binding site of *h*IMPDH2.

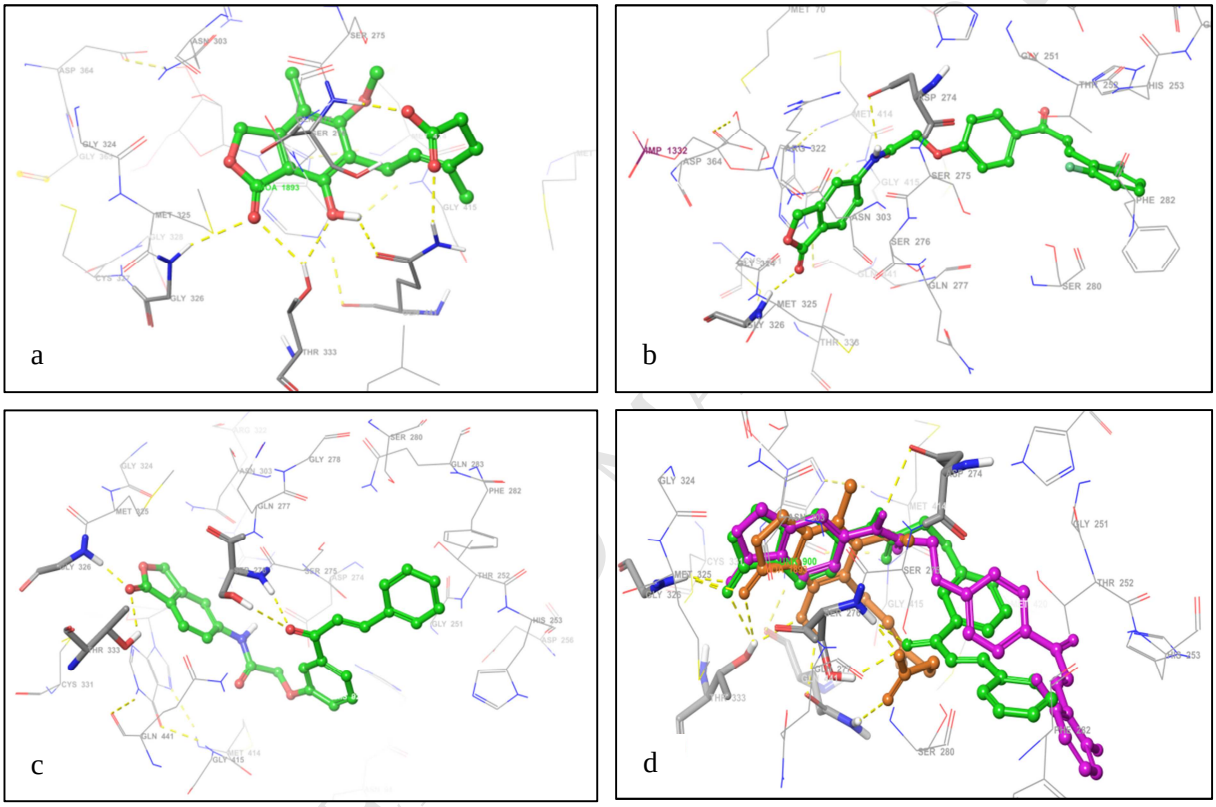

Figure 5. Binding mode of MPA and the hits into the cofactor-binding site of *h*IMPDH2 (PDB ID: 1JR1). The ligand is shown as ball-and-stick model while the *h*IMPDH2 residues are shown as line models coloured by the element. Yellow dotted-lines indicate H-bonding interactions. a) **MPA** formed H-bond with Ser276, Gly326, Thr333 and Gln441; b) **35** showed H-bonding interactions with Asp274 and Gly326; c) **41** was involved in H-bonding interactions with Ser276, Gly326 and Thr333; d) overlay of **MPA** (orange), **35** (purple) and **41** (green).

Table 4[a]. Results of the docking studies of the hits

Compound	XP G_{Score}	Glide E_{model} (kcal/mol)
MPA	-8.144	-75.421
41	-6.713	-77.132
35	-5.325	-76.915
30	-5.307	-72.782
33	-4.991	-72.020
43	-4.914	-76.495

[a] MPA docking results are shown for comparison

2.4. Solubility and Log $D_{7.4}$

Molecules with sufficient solubility (logS) and lipophilicity (e.g., $logD_{7.4}$) are obliging and seem to have a greater impact on ADMET properties during the drug discovery process. Solubility is an important parameter for the human intestinal absorption and subsequently to oral bioavailability and mostly command the route of drug administration. It is often expressed as log units of molar solubility (mol/L) or logS. The commended range for a molecule to be good oral bioavailable is -6 to 0.5 [50]. The most promising hits – **35** and **41**, exhibited experimental logS of -5.81. The distribution coefficient, on the other hand, has a crucial role to play in drug overall drug disposition. Hydrophilic molecules have higher solubility, but are less equipped to cross the cell membrane readily. A compound is hydrophilic, if logD < 0 and lipophilic, if logD > 0. Nearly ~85 % of the anticancer drugs have logD value ranging from -0.86 to 4.88 with a median of 2.57, while maximum lead candidates are hydrophobic in nature (logD = 3.15, median value) [50]. Given the absence of ionizable functional groups in the most promising hits, logD at physiological pH, i.e., pH 7.4 ($logD_{7.4}$) was determined to represent lipophilicity. The $logD_{7.4}$ values for compounds **35** and **41** were found 2.99 and 2.79, respectively.

3. Conclusions

The design strategy used in the present study, i.e., mimicking isobenzofuranone substructure and the *trans* configuration of MPA side chain, crucial for retaining the chemical features required for the *h*IMPDH2 inhibitory potential, yielded fruitful outcome. The synthesized compounds exhibited systematic SAR trends with respect to *in vitro* %

inhibition. The efforts successfully mapped the binding site of the enzyme in terms of the electronic nature, size and shape. The hits exhibited potent cytotoxicity against MDA-MB-231, DU145 and U87 MG and were relatively less toxic towards normal cells (NIH-3T3). Also, the most potent hits were significantly less toxic than MPA against hPBMC. The binding modes of the hits with hIMPDH2 cofactor-binding site clearly demonstrated conservation of the essential interactions of the core isobenzofuranone moiety while additional interactions by the distal end of the hits, i.e., chalcone portion. The identified hits illustrated improved cellular potency over MPA against the tested cancer cell lines. The series A hits were better than other two series as *h*IMPDH2 inhibitors. The interesting outcome of the present study is likely to guide further design and development of potential *h*IMPDH2 inhibitors as newer anticancer agents. Our concerted medicinal chemistry efforts thus, yielded potent lead molecules.

4. Experimental

4.1. General

All the chemicals utilized for the present study were purchased from the producers such as Acros Organics (Geel, Belgium), Alfa Aesar (Karlsruhe, Germany), Spectrochem (Mumbai, India), Sigma Aldrich (Steinheim, Germany) or Merck (Darmstadt, Germany) and used without further purification unless otherwise indicated. Solvents were used directly unless specified. All the reactions were carried out under dry N_2 atmosphere and progress of the reaction was monitored by thin layer chromatography (TLC) using an aluminium plate coated with silica gel 60 F_{254} (Merck Millipore, Billerica, MA, USA). All the title compounds were purified by column chromatography packed with silica gel of 230-400 mesh, 60 Å of Merck using a mixture of DCM/MeOH as eluent and the TLCs analyzed in a UV cabinet with an excitation wavelength of 254 nm. Melting points of the compounds was determined on Veego VMP DS (General Trading Co., India) and are uncorrected. FT-IR spectra were recorded on a Perkin Elmer RX1 instrument (Waltham, MA). The purity of all biologically evaluated compounds was determined using HPLC and found to be >95%. HPLC analysis was performed on Agilent 1220 Infinity system (Santa Clara, CA, USA). An isocratic mobile phase consisting of (A) Acetonitrile and (B) Water (80:20, v/v) was used with a C_{18} Kromasil® column (15 cm × 4.6 mm, 5 µ particle size, 100 Å pore size) (Bohus, Sweden), flow rate of 1 mL/min. The NMR spectra were recorded in DMSO-d_6 and tetramethylsilane (TMS) as internal standard. ^{1}H-NMR spectra were obtained on Bruker Advance 400 (400

MHz); chemical shifts are expressed in δ (ppm) Mass spectra (MS) were recorded on a Shimadzu 8040 LC-MS/MS system (Japan), using electrospray ionization (ESI) mode.

4.2. Synthesis

4.2.1. General procedure A: Synthesis of substituted chalcones (1-22) [46]. An aqueous solution of NaOH (20%, 5 mL) was added dropwise to a previously cooled mixture of selected acetophenone (5 mmol) and selected (hetero)aryl aldehydes (5 mmol) in EtOH (25 mL) under vigorous stirring. The mixture was stirred at RT for 24–72 hr. After completion of the reaction (as indicated by TLC), the mixture was poured onto crushed ice and acidified with dilute HCl. The precipitated product was filtered at suction and washed to neutral filtrate. The solid was recrystallized from EtOH to get crystalline product.

(*E*)-3-(3,4-dimethoxyphenyl)-1-(4-hydroxyphenyl)prop-2-en-1-one (1): The title compound was synthesized from 4-hydroxyacetophenone and 3,4-dimethoxybenzaldehyde as described in the general procedure A. Yield: 68%; mp: 204-206 °C.

(*E*)-1-(4-hydroxyphenyl)-3-(4-methoxyphenyl)prop-2-en-1-one (2): The title compound was synthesized from 4-hydroxyacetophenone and 4-methoxybenzaldehyde as described in the general procedure A. Yield: 72%; mp: 188-190 °C.

(*E*)-1-(4-hydroxyphenyl)-3-(thiophen-2-yl)prop-2-en-1-one (3): The title compound was synthesized from 4-hydroxyacetophenone and thiophene-2-carbaldehyde as described in the general procedure A. Yield: 69%; mp: 172-174 °C.

(*E*)-3-(2-chlorophenyl)-1-(4-hydroxyphenyl)prop-2-en-1-one (4): The title compound was synthesized from 4-hydroxyacetophenone and 2-chlorobenzaldehyde as described in the general procedure A. Yield: 78%; mp: 172-174 °C.

(*E*)-1-(4-hydroxyphenyl)-3-(3-methoxyphenyl)prop-2-en-1-one (5): The title compound was synthesized from 4-hydroxyacetophenone and 3-methoxybenzaldehyde as described in the general procedure A. Yield: 65%; mp: 162-164 °C.

(*E*)-1-(4-hydroxyphenyl)-3-(3,4,5-trimethoxyphenyl)prop-2-en-1-one (6): The title compound was synthesized from 4-hydroxyacetophenone and 3,4,5-trimethoxybenzaldehyde as3described in the general procedure A. Yield: 80%; mp: 238-240 °C.

(*E*)-3-(2,6-difluorophenyl)-1-(4-hydroxyphenyl)prop-2-en-1-one (7): The title compound was synthesized from 4-hydroxyacetophenone and 2,6-difluorobenzaldehyde as described in the general procedure A. Yield: 77%; mp: 198-200 °C.

(*E*)-1-(4-hydroxyphenyl)-3-(4-nitrophenyl)prop-2-en-1-one (8): The title compound was synthesized from 4-hydroxyacetophenone and 4-nitrobenzaldehyde as described in the general procedure A. Yield: 85%; mp: 250-252 °C.

(*E*)-1-(4-hydroxyphenyl)-3-phenylprop-2-en-1-one (9): The title compound was synthesized from 4-hydroxyacetophenone and benzaldehyde as described in the general procedure A. Yield: 70%; mp: 174-176 °C.

(*E*)-3-(furan-2-yl)-1-(4-hydroxyphenyl)prop-2-en-1-one (10): The title compound was synthesized from 4-hydroxyacetophenone and furan-2-carbaldehyde as described in the general procedure A. Yield: 68%; mp: 162-164 °C.

(*E*)-3-(3,4-dimethoxyphenyl)-1-(3-hydroxyphenyl)prop-2-en-1-one (11): The title compound was synthesized from 3-hydroxyacetophenone and 3,4-dimethoxybenzaldehyde as described in the general procedure A. Yield: 70%; mp: 86-88 °C.

(*E*)-1-(3-hydroxyphenyl)-3-(3,4,5-trimethoxyphenyl)prop-2-en-1-one (12): The title compound was synthesized from 3-hydroxyacetophenone and 3,4,5-trimethoxybenzaldehyde as described in the general procedure A. Yield: 80%; mp: 174-176 °C.

(*E*)-1-(3-hydroxyphenyl)-3-phenylprop-2-en-1-one (13): The title compound was synthesized from 3-hydroxyacetophenone and benzaldehyde as described in the general procedure A. Yield: 67%; mp: 130-132 °C.

(*E*)-1-(4-hydroxy-3-methoxyphenyl)-3-(3,4,5-trimethoxyphenyl)prop-2-en-1-one(14):
The title compound was synthesized from 4-hydroxy-3-methoxyacetophenone and 3,4,5-trimethoxybenzaldehyde as described in the general procedure A. Yield: 64%; mp: 188-190 °C.

(*E*)-1-(4-fluorophenyl)-3-(4-hydroxyphenyl)prop-2-en-1-one (15): The title compound was synthesized from 4-fluoroacetophenone and 4-hydroxybenzaldehyde as described in the general procedure A. Yield: 73%; mp: 188-190 °C.

(*E*)-3-(4-chlorophenyl)-1-(4-hydroxyphenyl)prop-2-en-1-one (16): The title compound was synthesized from 4-hydroxyacetophenone and 4-chlorobenzaldehyde as described in the general procedure A. Yield: 63%; mp: 186-188 °C.

(*E*)-3-(4-(benzyloxy)phenyl)-1-(4-hydroxyphenyl)prop-2-en-1-one (17): The title compound was synthesized from 4-hydroxyacetophenone and 4-(benzyloxy)benzaldehyde as described in the general procedure A. Yield: 68%; mp: 180-182 °C.

(*E*)-3-(4-(2,4-dichlorobenzyloxy)phenyl)-1-(4-hydroxyphenyl)prop-2-en-1-one (18): The title compound was synthesized from 4-hydroxyacetophenone and 4-(2,4-dichlorobenzyloxy)benzaldehyde as described in the general procedure A. Yield: 70%; mp: 202-204 °C.

(*E*)-3-(4-(4-chlorobenzyloxy)phenyl)-1-(4-hydroxyphenyl)prop-2-en-1-one (19): The title compound was synthesized from 4-hydroxyacetophenone and 4-(4-chlorobenzyloxy)-benzaldehyde as described in the general procedure A. Yield: 67%; mp: 200-202 °C.

(*E*)-3-(4-ethoxyphenyl)-1-(4-hydroxyphenyl)prop-2-en-1-one (20): The title compound was synthesized from 4-hydroxyacetophenone and 4-ethoxybenzaldehyde as described in the general procedure A. Yield: 62%; mp: 144-146 °C.

(*E*)-1-(4-hydroxyphenyl)-3-(4-propoxyphenyl)prop-2-en-1-one (21): The title compound was synthesized from 4-hydroxyacetophenone and 4-propoxybenzaldehyde as described in the general procedure A. Yield: 65%; mp: 162-164 °C.

(*E*)-3-(4-butoxyphenyl)-1-(4-hydroxyphenyl)prop-2-en-1-one (22): The title compound was synthesized from 4-hydroxyacetophenone and 4-butoxybenzaldehyde as described in the general procedure A. Yield: 64%; mp: 148-150 °C.

4.2.2. General procedure B: Synthesis of substituted chloroacetamides (26-28) [47]. To a mixture of amine (1 eq.) and TEA (1.2 eq.) in dry THF was added chloroacetyl chloride (1.1 eq.) dropwise at 0 °C. After completion of reaction, triethylammonium chloride was filtered off and the filtrate was concentrated under vacuum and quenched with water. The solid obtained was filtered at suction and washed to neutral filtrate, air dried and used without any further purification.

2-chloro-*N*-(1-oxo-1,3-dihydroisobenzofuran-5-yl)acetamide (26): The title compound was synthesized from **23** (3 g, 20.1 mmol), TEA (3.36 mL, 24.12 mmol) and chloroacetyl chloride (1.76 mL, 22.11 mmol) as described in the general procedure B to yield **26** as a light brown solid. Yield: 90%; mp: 218-220 °C.

2-chloro-*N*-(3,4-dimethoxyphenyl)acetamide (27): The title compound was synthesized from **24** (3 g, 19.6 mmol), TEA (3.28 mL, 23.5 mmol) and chloroacetyl chloride (1.71 mL, 21.54 mmol) as described in the general procedure B to yield **27** as a dark grey solid. Yield: 88%; mp: 182-184 °C.

***N*-(benzo[*d*][1,3]dioxol-5-ylmethyl)-2-chloroacetamide (28):** The title compound was synthesized from **25** (3 g, 19.85 mmol), TEA (3.32 mL, 23.82 mmol) and chloroacetyl chloride (1.74 mL, 21.83 mmol) as described in the general procedure B to yield **28** as a brown solid. Yield: 85%; mp: 106-108 °C.

4.2.3. General procedure C: Synthesis of final compounds (29-65) [47]. A solution chloroacetamides (**26** or **27** or **28**, 1 eq.), anhydrous K_2CO_3 (3 eq.), and appropriate chalcone (**1-22**, 1 eq.) in dry DMF (4 mL) was stirred for 16 hr at 25 °C. After completion of the reaction, the reaction mixture was quenched with brine (50 mL). The precipitated product was filtered off, washed with water and dried under vacuum. The crude product was further purified by column chromatography using DCM:MeOH (95:5) as mobile phase.

(*E*)-2-(4-(3-(3,4-dimethoxyphenyl)acryloyl)phenoxy)-N-(1-oxo-1,3-dihydroisobenzofuran-5-yl)acetamide (29): It was synthesized from **26** (0.1 g, 0.44 mmol), K_2CO_3 (0.18 g, 1.33 mmol), and **1** (0.12 g, 0.44 mmol) as described in the general procedure C to yield **29** as a white solid. Yield: 68%; TLC R_f = 0.46 (DCM:MeOH, 95:5); purity (HPLC): >99%; mp: 202-204 °C; ^{1}H-NMR (DMSO-d_6, 400 MHz) δ 10.7 (brs, 1H), 8.17 (d, *J* = 8.4 Hz, 2H), 8.05 (s, 1H), 7.87-7.76 (m, 2H), 7.73-7.62 (m, 2H), 7.52 (s, 1H), 7.36 (d, *J* = 8.3 Hz, 1H), 7.14 (d, *J* = 8.5 Hz, 2H), 7.01 (d, *J* = 8.3 Hz, 1H), 5.36 (s, 2H), 4.91 (s, 2H), 3.84 (s, 3H), 3.80 (s, 3H); MS (ESI) *m/z*: 474 $[M+H]^+$.

(*E*)-2-(4-(3-(4-methoxyphenyl)acryloyl)phenoxy)-N-(1-oxo-1,3-dihydroisobenzofuran-5-yl)acetamide (30): It was synthesized from **26** (0.1 g, 0.44 mmol), K_2CO_3 (0.18 g, 1.33 mmol), and **2** (0.11 g, 0.44 mmol) as described in the general procedure C to yield **30** as a white solid. Yield: 65%; TLC R_f = 0.48 (DCM:MeOH, 95:5); purity (HPLC): 98.03%; mp: 218-220 °C; ^{1}H-NMR (DMSO-d_6, 400 MHz) δ 10.68 (s, 1H), 8.16 (d, *J* = 8.6 Hz, 2H), 8.06 (s, 1H), 7.87-

7.76 (m, 4H), 7.75-7.63 (m, 2H), 7.14 (d, *J* = 8.6 Hz, 2H), 7.00 (d, *J* = 8.5 Hz, 2H), 5.37 (s, 2H), 4.92 (s, 2H), 3.81 (s, 3H); ^{13}C-NMR (DMSO-d_6, 100 MHz) δ 187.25, 170.14, 166.89, 161.46, 161.21, 148.91, 143.63, 143.23, 131.27, 130.69, 130.64, 127.39, 125.79, 120.16, 119.69, 119.43, 114.61, 114.35, 112.34, 69.56, 67.05, 55.33; MS (ESI) *m/z*: 444 $[M+H]^+$.

(*E*)-N-(1-oxo-1,3-dihydroisobenzofuran-5-yl)-2-(4-(3-(thiophen-2-yl)acryloyl)phenoxy)-acetamide (31): It was synthesized from **26** (0.1 g, 0.44 mmol), K_2CO_3 (0.18 g, 1.33 mmol), and **3** (0.1 g, 0.44 mmol) as described in the general procedure C to yield **31** as a white solid. Yield: 62%; TLC R_f = 0.51 (DCM:MeOH, 95:5); purity (HPLC): >99%; mp: 248-250 °C; ^{1}H-NMR (DMSO-d_6, 400 MHz) δ 10.7 (brs, 1H), 8.11 (d, *J* = 8.8 Hz, 2H), 8.05 (s, 1H), 7.87 (d, *J* = 15.2 Hz, 1H), 7.81-7.74 (m, 2H), 7.72-7.62 (m, 2H), 7.57 (d, *J* = 15.3 Hz, 1H), 7.22-7.09 (m, 3H), 5.36 (s, 2H), 4.91 (s, 2H); MS (ESI) *m/z*: 420 $[M+H]^+$.

(*E*)-2-(4-(3-(2-chlorophenyl)acryloyl)phenoxy)-N-(1-oxo-1,3-dihydroisobenzofuran-5-yl)acetamide (32): It was synthesized from **26** (0.1 g, 0.44 mmol), K_2CO_3 (0.18 g, 1.33 mmol), and **4** (0.11 g, 0.44 mmol) as described in the general procedure C to yield **32** as a white solid. Yield: 65%; TLC R_f = 0.52 (DCM:MeOH, 95:5); purity (HPLC): 98.97%; mp: >300 °C; ^{1}H-NMR (DMSO-d_6, 400 MHz) δ 10.82 (brs, 1H), 8.22-8.18 (m, 3H), 8.07 (s, 1H), 8.00 (s, 2H), 7.81 (d, *J* = 8.4 Hz, 1H), 7.72 (d, *J* = 6.7 Hz, 1H), 7.60-7.51 (m, 1H), 7.57-7.44 (m, 2H), 7.17-7.15 (m, 2H), 5.37 (s, 2H), 4.95 (s, 2H); MS (ESI) *m/z*: 448 $[M+H]^+$.

(*E*)-2-(4-(3-(3-methoxyphenyl)acryloyl)phenoxy)-N-(1-oxo-1,3-dihydroisobenzofuran-5-yl)acetamide (33): It was synthesized from **26** (0.1 g, 0.44 mmol), K_2CO_3 (0.18 g, 1.33 mmol), and **5** (0.11 g, 0.44 mmol) as described in the general procedure C to yield **33** as a white solid. Yield: 67%; TLC R_f = 0.46 (DCM:MeOH, 95:5); purity (HPLC): >99%; mp: 196-198 °C; ^{1}H-NMR (DMSO-d_6, 400 MHz) δ 10.74 (brs, 1H), 8.19 (d, *J* = 8.4 Hz, 2H), 8.05 (s, 1H), 7.94 (d, *J* = 15.0 Hz, 1H), 7.80 (d, *J* = 8.7 Hz, 1H), 7.68 (d, *J* = 10.8 Hz, 2H), 7.55-7.27 (m, 3H), 7.14 (d, *J* = 8.6 Hz, 2H), 7.04-6.97 (m, 1H), 5.36 (s, 2H), 4.92 (s, 2H), 3.82 (s, 3H); ^{13}C-NMR (DMSO-d_6, 100 MHz) δ 187.38, 170.16, 166.91, 161.69, 159.61, 148.90, 143.87, 143.24, 136.16, 130.98, 130.89, 129.86, 125.77, 122.23, 121.56, 120.17, 119.59, 116.48, 114.66, 113.29, 112.37, 69.54, 67.10, 55.26; MS (ESI) *m/z*: 444 $[M+H]^+$.

(*E*)-N-(1-oxo-1,3-dihydroisobenzofuran-5-yl)-2-(4-(3-(3,4,5-trimethoxyphenyl)acryloyl) phenoxy)acetamide (34): It was synthesized from **26** (0.1 g, 0.44 mmol), K_2CO_3 (0.18 g, 1.33 mmol), and **6** (0.14 g, 0.44 mmol) as described in the general procedure C to yield **34** as a white

solid. Yield: 68%; TLC R_f = 0.39 (DCM:MeOH, 95:5); purity (HPLC): 97.70%; mp: 238-240 °C; ^{1}H-NMR (DMSO-d_6, 400 MHz) δ 10.75 (brs, 1H), 8.22-8.15 (m, 2H), 8.04 (s, 1H), 7.89 (d, *J* = 15.5 Hz, 1H), 7.79 (d, *J* = 8.4 Hz, 1H), 7.72-7.61 (m, 2H), 7.21 (s, 2H), 7.14 (d, *J* = 8.8 Hz, 2H), 5.36 (s, 2H), 4.91 (s, 2H), 3.85 (s, 6H), 3.70 (s, 3H); MS (ESI) *m/z*: 504 $[M+H]^+$.

(*E*)-2-(4-(3-(2,6-difluorophenyl)acryloyl)phenoxy)-N-(1-oxo-1,3-dihydroisobenzofuran-5-yl)acetamide (35): It was synthesized from **26** (0.1 g, 0.44 mmol), K_2CO_3 (0.18 g, 1.33 mmol), and **7** (0.11 g, 0.44 mmol) as described in the general procedure C to yield **35** as a white solid. Yield: 65%; TLC R_f = 0.57 (DCM:MeOH, 95:5); purity (HPLC): >99%; mp: 242-244 °C; ^{1}H-NMR (DMSO-d_6, 400 MHz) δ 10.06 (brs, 1H), 8.07-8.03 (m, 3H), 7.86 (d, *J* = 16.0 Hz, 1H), 7.77 (d, *J* = 8.4 Hz, 1H), 7.67-7.63 (m, 2H), 7.58-7.50 (m, 1H), 7.25 (t, *J* = 8.9 Hz, 2H), 7.15 (d, *J* = 8.4 Hz, 2H), 5.34 (s, 2H), 4.90 (s, 2H); ^{13}C-NMR (DMSO-d_6, 100 MHz) δ 187.24, 170.17, 166.86, 162.31, 161.97, 159.72, 148.90, 144.00, 132.28, 130.81, 130.45, 128.56, 127.37, 125.75, 120.20, 119.52, 114.90, 112.46, 112.37, 112.22, 112.07, 69.55, 67.08; MS (ESI) *m/z*: 450 $[M+H]^+$.

(*E*)-2-(4-(3-(4-nitrophenyl)acryloyl)phenoxy)-N-(1-oxo-1,3-dihydroisobenzofuran-5-yl) acetamide (36): It was synthesized from **26** (0.1 g, 0.44 mmol), K_2CO_3 (0.18 g, 1.33 mmol), and **8** (0.11 g, 0.44 mmol) as described in the general procedure C to yield **36** as a white solid. Yield: 70%; TLC R_f = 0.39 (DCM:MeOH, 95:5); purity (HPLC): >99%; mp: 250-254 °C; ^{1}H-NMR (DMSO-d_6, 400 MHz) δ 10.71 (brs, 1H), 8.27 (d, *J* = 8.4 Hz, 2H), 8.21 (d, *J* = 8.5 Hz, 2H), 8.17-8.103 (m, 3H), 8.05 (s, 1H), 7.80-7.76 (m, 2H), 7.70 (d, *J* = 8.4 Hz, 1H), 7.16 (d, *J* = 8.5 Hz, 2H), 5.36 (s, 2H), 4.93 (s, 2H); MS (ESI) *m/z*: 459 $[M+H]^+$.

(*E*)-2-(4-cinnamoylphenoxy)-N-(1-oxo-1,3-dihydroisobenzofuran-5-yl)acetamide (37): The title compound was synthesized from **26** (0.1 g, 0.44 mmol), K_2CO_3 (0.18 g, 1.33 mmol), and **9** (0.09 g, 0.44 mmol) as described in the general procedure C to yield **37** as a white solid. Yield: 66%; TLC R_f = 0.60 (DCM:MeOH, 95:5); purity (HPLC): 98.34%; mp: 228-230 °C; ^{1}H-NMR (DMSO-d_6, 400 MHz) δ 10.78 (brs, 1H), 8.18 (d, *J* = 8.8 Hz, 2H), 8.05 (s, 1H), 7.95 (d, *J* = 15.6 Hz, 1H), 7.87 (d, *J* = 6.6 Hz, 2H), 7.79 (d, *J* = 8.4 Hz, 1H), 7.75-7.66 (m, 2H), 7.50-7.40 (m, 3H), 7.14 (d, *J* = 8.8 Hz, 2H), 5.36 (s, 2H), 4.92 (s, 2H); MS (ESI) *m/z*: 414 $[M+H]^+$.

(*E*)-2-(4-(3-(furan-2-yl)acryloyl)phenoxy)-N-(1-oxo-1,3-dihydroisobenzofuran-5-yl) acetamide (38): It was synthesized from **26** (0.1 g, 0.44 mmol), K_2CO_3 (0.18 g, 1.33 mmol), and

10 (0.09 g, 0.44 mmol) as described in the general procedure C to yield **38** as a white solid. Yield: 67%; TLC R_f = 0.49 (DCM;MeOH, 95:5); purity (HPLC): >99%; mp: >300 °C; ^{1}H-NMR (DMSO-d_6, 400 MHz) δ 10.70 (s, 1H), 8.10-8.06 (m, 3H), 7.90 (s, 1H), 7.81 (d, *J* = 8.3 Hz, 1H), 7.71 (d, *J* = 8.4 Hz, 1H), 7.54 (s, 2H), 7.13 (d, *J* = 8.9 Hz, 2H), 7.08 (d, *J* = 3.4 Hz, 1H), 6.68 (d, *J* = 3.5 Hz, 1H), 5.37 (s, 2H), 4.92 (s, 2H); MS (ESI) *m/z*: 404 $[M+H]^+$.

(*E*)-2-(3-(3-(3,4-dimethoxyphenyl)acryloyl)phenoxy)-N-(1-oxo-1,3-dihydroisobenzofuran-5-yl)acetamide (39): It was synthesized from **26** (0.1 g, 0.44 mmol), K_2CO_3 (0.18 g, 1.33 mmol), and **11** (0.12 g, 0.44 mmol) as described in the general procedure C to yield **39** as a white solid. Yield: 69%; TLC R_f = 0.47 (DCM:MeOH, 95:5); purity (HPLC): 99%; mp: 184-186 °C; ^{1}H-NMR (DMSO-d_6, 400 MHz) δ 10.71 (brs, 1H), 8.07 (s, 1H), 7.82-7.77 (m, 3H), 7.71-7.67 (m, 3H), 7.52 (d, *J* = 2.9 Hz, 2H), 7.38 (d, *J* = 8.4 Hz, 1H), 7.30 (d, *J* = 8.4 Hz, 1H), 7.00 (d, *J* = 8.4 Hz, 1H), 5.36 (s, 2H), 4.89 (s, 2H), 3.84 (s, 3H), 3.81 (s, 3H); MS (ESI) *m/z*: 474 $[M+H]^+$.

(*E*)-N-(1-oxo-1,3-dihydroisobenzofuran-5-yl)-2-(3-(3-(3,4,5-trimethoxyphenyl)acryloyl)-phenoxy)acetamide (40): It was synthesized from **26** (0.1 g, 0.44 mmol), K_2CO_3 (0.18 g, 1.33 mmol), and **12** (0.14 g, 0.44 mmol) as described in the general procedure C to yield **40** as a white solid. Yield: 70%; TLC R_f = 0.41 (DCM:MeOH, 95:5); purity (HPLC): >99%; mp: 222-224 °C; ^{1}H-NMR (DMSO-d_6, 400 MHz) δ 10.72 (brs, 1H), 8.06 (s, 1H), 7.88-7.78 (m, 3H), 7.70-7.68 (m, 3H), 7.53 (t, *J* = 7.9 Hz, 1H), 7.31 (d, *J* = 8.2 Hz, 1H), 7.23 (s, 2H), 5.36 (s, 2H), 4.89 (s, 2H), 3.85 (s, 6H), 3.70 (s, 3H); MS (ESI) *m/z*: 504 $[M+H]^+$.

(*E*)-2-(3-cinnamoylphenoxy)-N-(1-oxo-1,3-dihydroisobenzofuran-5-yl)acetamide (41): It was synthesized from **26** (0.1 g, 0.44 mmol), K_2CO_3 (0.18 g, 1.33 mmol), and **13** (0.09 g, 0.44 mmol) as described in the general procedure C to yield **41** as a white solid. Yield: 67%; TLC R_f = 0.59 (DCM;MeOH, 95:5); purity (HPLC): >99%; mp: 160-162 °C; ^{1}H-NMR (DMSO-d_6, 400 MHz) δ 10.75 (brs, 1H), 8.07 (s, 1H), 7.93-7.86 (m, 3H), 7.82-7.78 (m, 2H), 7.75-7.69 (m, 3H), 7.52 (t, *J* = 7.9 Hz, 1H), 7.45-7.42 (m, 3H), 7.32 (d, *J* =8.2 Hz, 1H), 5.36 (s, 2H), 4.90 (s, 2H); ^{13}C-NMR (DMSO-d_6, 100 MHz) δ 188.80, 170.19, 167.25, 158.07, 148.92, 144.24, 143.87, 138.95, 134.58, 130.69, 130.04, 128.90, 125.78, 122.07, 121.76, 120.22, 119.84, 119.60, 113.92, 112.40, 69.57, 67.21; MS (ESI) *m/z*: 414 $[M+H]^+$.

(*E*)-2-(2-methoxy-4-(3-(3,4,5-trimethoxyphenyl)acryloyl)phenoxy)-N-(1-oxo-1,3-dihydroisobenzofuran-5-yl)acetamide (42): It was synthesized from **26** (0.1 g, 0.44 mmol),

K_2CO_3 (0.18 g, 1.33 mmol), and **14** (0.15 g, 0.44 mmol) as described in the general procedure C to yield **42** as a white solid. Yield: 68%; TLC R_f = 0.38 (DCM:MeOH, 95:5); purity (HPLC): >99%; mp: >300 °C; ^{1}H-NMR (DMSO-d_6, 400 MHz) δ 10.91 (brs, 1H), 8.04 (s, 1H), 7.92-7.84 (m, 2H), 7.80 (d, *J* = 8.4 Hz, 1H), 7.69-7.62 (m, 3H), 7.21 (s, 2H), 7.06 (d, *J* = 8.5 Hz, 1H), 5.36 (s, 2H), 4.94 (s, 2H), 3.90 (s, 3H), 3.84 (s, 6H), 3.69 (s, 3H); MS (ESI) *m/z*: 534 $[M+H]^+$.

(*E*)-2-(4-(3-(4-fluorophenyl)-3-oxoprop-1-enyl)phenoxy)-N-(1-oxo-1,3-dihydroisobenzofuran-5-yl)acetamide (43): It was synthesized from **26** (0.1 g, 0.44 mmol), K_2CO_3 (0.18 g, 1.33 mmol), and **15** (0.11 g, 0.44 mmol) as described in the general procedure C to yield **43** as a white solid. Yield: 63%; TLC R_f = 0.58 (DCM:MeOH, 95:5); purity (HPLC): >99%; mp: 232-234 °C; ^{1}H-NMR (DMSO-d_6, 400 MHz) δ 10.78 (brs, 1H), 8.23 (d, *J* = 8.7 Hz, 2H), 8.07 (s, 1H), 7.89 (d, *J* = 2.0 Hz, 1H), 7.86 (d, *J* = 5.7 Hz, 1H), 7.80 (d, *J* = 8.2 Hz, 2H), 7.73 (d, *J* = 3.4 Hz, 1H), 7.70 (d, *J* = 3.8 Hz, 1H), 7.38 (t, *J* = 8.8 Hz, 2H), 7.08 (d, *J* = 8.8 Hz, 2H), 5.37 (s, 2H), 4.88 (s, 2H); ^{13}C-NMR (DMSO-d_6, 100 MHz) δ 187.53, 170.17, 167.09, 166.19, 159.83, 148.91, 143.94, 143.74, 134.43, 131.42, 131.33, 130.79, 127.93, 125.78, 120.14, 119.67, 115.83, 115.61, 115.08, 112.34, 69.57, 67.06; MS (ESI) *m/z*: 432 $[M+H]^+$.

(*E*)-2-(4-(3-(4-chlorophenyl)acryloyl)phenoxy)-N-(1-oxo-1,3-dihydroisobenzofuran-5-yl)acetamide (44): It was synthesized from **26** (0.1 g, 0.44 mmol), K_2CO_3 (0.18 g, 1.33 mmol), and **16** (0.11 g, 0.44 mmol) as described in the general procedure C to yield **44** as a white solid. Yield: 61%; TLC R_f = 0.49 (DCM:MeOH, 95:5); purity (HPLC): >99%; mp: 288-290 °C; ^{1}H-NMR (DMSO-d_6, 400 MHz) δ 10.78 (s, 1H), 8.19 (d, *J* = 8.9 Hz, 2H), 8.07 (s, 1H), 7.99-7.90 (m, 3H), 7.81 (d, *J* = 8.4 Hz, 1H), 7.73-7.67 (m, 2H), 7.51 (d, *J* = 8.5 Hz, 2H), 7.15 (d, *J* = 8.9 Hz, 2H), 5.37 (s, 2H), 4.94 (s, 2H); MS (ESI) *m/z*: 448 $[M+H]^+$.

(*E*)-2-(4-(3-(4-(benzyloxy)phenyl)acryloyl)phenoxy)-N-(1-oxo-1,3-dihydroisobenzofuran-5-yl)acetamide (45): It was synthesized from **26** (0.1 g, 0.44 mmol), K_2CO_3 (0.18 g, 1.33 mmol), and **17** (0.15 g, 0.44 mmol) as described in the general procedure C to yield **45** as a white solid. Yield: 65%; TLC R_f = 0.52 (DCM:MeOH, 95:5); purity (HPLC): >99%; mp: 242-244 °C; ^{1}H-NMR (DMSO-d_6, 400 MHz) δ 10.68 (s, 1H), 8.17 (d, *J* = 8.5 Hz, 2H), 8.07 (s, 1H), 7.84-7.79 (m, 4H), 7.72-7.65 (m, 2H), 7.46 (d, *J* = 7.5 Hz, 2H), 7.39 (t, *J* = 7.4 Hz, 2H), 7.33 (t, *J* = 7.2 Hz, 1H), 7.14 (d, *J* = 8.5 Hz, 2H), 7.08 (d, *J* = 8.3 Hz, 2H), 5.37 (s, 2H), 5.17 (s, 2H), 4.93 (s, 2H); MS (ESI) *m/z*: 520 $[M+H]^+$.

(*E*)-2-(4-(3-(4-(2,4-dichlorobenzyloxy)phenyl)acryloyl)phenoxy)-N-(1-oxo-1,3-dihydro-isobenzofuran-5-yl)acetamide (46): It was synthesized from **26** (0.1 g, 0.44 mmol), K_2CO_3 (0.18 g, 1.33 mmol), and **18** (0.18 g, 0.44 mmol) as described in the general procedure C to yield **46** as a white solid. Yield: 66%; TLC R_f = 0.54 (DCM:MeOH, 95:5); purity (HPLC): >99%; mp: 228-230 °C; ^{1}H-NMR (DMSO-d_6, 400 MHz) δ 10.69 (s, 1H), 8.17 (d, *J* = 8.5 Hz, 2H), 8.07 (s, 1H), 7.86-7.80 (m, 4H), 7.72-7.62 (m, 4H), 7.49 (d, *J* = 2.2, 8.3 Hz, 1H), 7.15-7.09 (m, 4H), 5.37 (s, 2H), 5.21 (s, 2H), 4.93 (s, 2H); MS (ESI) *m/z*: 588 $[M+H]^+$.

(*E*)-2-(4-(3-(4-(4-chlorobenzyloxy)phenyl)acryloyl)phenoxy)-N-(1-oxo-1,3-dihydro-isobenzofuran-5-yl)acetamide (47): It was synthesized from **26** (0.1 g, 0.44 mmol), K_2CO_3 (0.18 g, 1.33 mmol), and **19** (0.16 g, 0.44 mmol) as described in the general procedure C to yield **47** as a white solid. Yield: 62%; TLC R_f = 0.52 (DCM:MeOH, 95:5); purity (HPLC): >99%; mp: >300 °C; ^{1}H-NMR (DMSO-d_6, 400 MHz)) δ 10.71 (s, 1H), 8.16 (d, *J* = 8.8 Hz, 2H), 8.07 (s, 1H), 7.85-7.80 (m, 4H), 7.72-7.65 (m, 2H), 7.50-7.42 (m, 4H), 7.14 (d, *J* = 8.8 Hz, 2H), 7.08 (d, *J* = 8.5 Hz, 2H), 5.37 (s, 2H), 5.18 (s, 2H), 4.93 (s, 2H); MS (ESI) *m/z*: 554 $[M+H]^+$.

(*E*)-2-(4-(3-(4-ethoxyphenyl)acryloyl)phenoxy)-N-(1-oxo-1,3-dihydroisobenzo-furan-5-yl)acetamide (48): It was synthesized from **26** (0.1 g, 0.44 mmol), K_2CO_3 (0.18 g, 1.33 mmol), and **20** (0.12 g, 0.44 mmol) as described in the general procedure C to yield **48** as a white solid. Yield: 58%; TLC R_f = 0.55 (DCM:MeOH, 95:5); purity (HPLC): >99%; mp: >300 °C; ^{1}H-NMR (DMSO-d_6, 400 MHz) δ 11.05 (s, 1H), 8.16 (d, *J* = 8.9 Hz, 2H), 8.09 (s, 1H), 7.83-7.75 (m, 5H), 7.67 (d, *J* = 15.5 Hz, 1H), 7.13 (d, *J* = 8.9 Hz, 2H), 6.98 (d, *J* = 8.8 Hz, 2H), 5.37 (s, 2H), 4.97 (s, 2H), 4.08 (q, *J* = 6.9 Hz, 2H), 1.33 (t, *J* = 7.0 Hz, 3H); MS (ESI) *m/z*: 458 $[M+H]^+$.

(*E*)-N-(1-oxo-1,3-dihydroisobenzofuran-5-yl)-2-(4-(3-(4-propoxyphenyl)acryloyl)-phenoxy)acetamide (49): It was synthesized from **26** (0.1 g, 0.44 mmol), K_2CO_3 (0.18 g, 1.33 mmol), and **21** (0.12 g, 0.44 mmol) as described in the general procedure C to yield **49** as a white solid. Yield: 57%; TLC R_f = 0.57 (DCM:MeOH, 95:5); purity (HPLC): >99%; mp: >300 °C; ^{1}H-NMR (DMSO-d_6, 400 MHz) δ 10.68 (s, 1H), 8.16 (d, *J* = 8.4 Hz, 2H), 8.06 (s, 1H), 7.82-7.78 (m, 4H), 7.72-7.65 (m, 2H), 7.14 (d, *J* = 8.5 Hz, 2H), 6.99 (d, *J* = 8.3 Hz, 2H), 5.37 (s, 2H), 4.92 (s, 2H), 3.98 (t, *J* = 6.5 Hz, 2H), 3.16 (d, *J* = 5.1 Hz, 1H), 1.73 (q, *J* = 7.0 Hz, 2H), 0.98 (t, *J* = 7.4 Hz, 3H); MS (ESI) *m/z*: 472 $[M+H]^+$.

(*E*)-2-(4-(3-(4-butoxyphenyl)acryloyl)phenoxy)-N-(1-oxo-1,3-dihydroisobenzo-furan-5-yl)acetamide (50): It was synthesized from **26** (0.1 g, 0.44 mmol), K_2CO_3 (0.18 g, 1.33 mmol), and **22** (0.13 g, 0.44 mmol) as described in the general procedure C to yield **50** as a white solid. Yield: 55%; TLC R_f = 0.57 (DCM:MeOH, 95:5); purity (HPLC): >99%; mp: >300 °C; ^{1}H-NMR (DMSO-d_6, 400 MHz) δ 10.73 (s, 1H), 8.16 (d, *J* = 8.6 Hz, 2H), 8.06 (s, 1H), 7.82-7.78 (m, 4H), 7.70-7.63 (m, 2H), 7.13 (d, *J* = 8.6 Hz, 2H), 6.99 (d, *J* = 8.4 Hz, 2H), 5.36 (s, 2H), 4.91 (s, 2H), 4.02 (t, *J* = 6.5 Hz, 2H), 1.70 (d, *J* = 8.5 Hz, 2H), 1.43 (q, *J* = 7.5 Hz, 2H), 0.93 (t, *J* = 7.4 Hz, 3H).; MS (ESI) *m/z*: 486 $[M+H]^+$.

(*E*)-N-(3,4-dimethoxyphenyl)-2-(4-(3-(4-methoxyphenyl)acryloyl)phenoxy)acetamide (51): It was synthesized from **27** (0.1 g, 0.44 mmol), K_2CO_3 (0.18 g, 1.33 mmol), and **2** (0.11 g, 0.44 mmol) as described in the general procedure C to yield **51** as a grey solid. Yield: 54%; TLC R_f = 0.54 (DCM:MeOH, 95:5); purity (HPLC): 98.10%; mp: 188-190 °C; ^{1}H-NMR (DMSO-d_6, 400 MHz) δ 10.03 (s, 1H), 8.17 (d, *J* = 8.4 Hz, 2H), 7.84-7.80 (m, 3H), 7.68 (d, *J* = 15.5 Hz, 1H), 7.33 (d, *J* = 2.4 Hz, 1H), 7.18-7.13 (m, 3H), 7.01 (d, *J* = 8.3 Hz, 2H), 6.90 (d, *J* = 8.7 Hz, 1H), 4.80 (s, 2H), 3.81 (s, 3H), 3.71 (d, *J* = 2.3 Hz, 6H); MS (ESI) *m/z*: 448 $[M+H]^+$.

(*E*)-N-(3,4-dimethoxyphenyl)-2-(4-(3-(3-methoxyphenyl)acryloyl)phenoxy)acetamide (52): It was synthesized from **27** (0.1 g, 0.44 mmol), K_2CO_3 (0.18 g, 1.33 mmol), and **5** (0.11 g, 0.44 mmol) as described in the general procedure C to yield **52** as a grey solid. Yield: 57%; TLC R_f = 0.55 (DCM:MeOH, 95:5); purity (HPLC): 98.39%; mp: 290-292 °C; ^{1}H-NMR (DMSO-d_6, 400 MHz)) δ 10.02 (s, 1H), 8.19 (d, *J* = 8.5 Hz, 2H), 7.95 (d, *J* = 15.7 Hz, 1H), 7.68 (d, *J* = 15.5 Hz, 1H), 7.47 (s, 1H), 7.42 (d, *J* = 7.4 Hz, 1H), 7.37-7.32 (m, 2H), 7.15-7.13 (m, 3H), 7.01 (d, *J* = 7.9 Hz, 1H), 6.90 (d, *J* = 8.7 Hz, 1H), 4.81 (s, 2H), 3.82 (d, *J* = 1.4 Hz, 3H), 3.71 (d, *J* = 1.7 Hz, 6H); MS (ESI) *m/z*: 448 $[M+H]^+$.

(*E*)-N-(3,4-dimethoxyphenyl)-2-(3-(3-(3,4-dimethoxyphenyl)acryloyl)phenoxy)acetamide (53): It was synthesized from **27** (0.1 g, 0.44 mmol), K_2CO_3 (0.18 g, 1.33 mmol), and **11** (0.13 g, 0.44 mmol) as described in the general procedure C to yield **53** as a grey solid. Yield: 55%; TLC R_f = 0.52 (DCM:MeOH, 95:5); purity (HPLC): >99%; mp: >300 °C; ^{1}H-NMR (DMSO-d_6, 400 MHz) δ 10.25 (s, 1H), 7.83-7.79 (m, 2H), 7.71-7.67 (m, 2H), 7.54-7.52 (m, 1H), 7.51-7.49 (m, 1H), 7.40-7.36 (m, 2H), 7.30 (d, *J* = 8.2 Hz, 1H), 7.20 (d, *J* = 2.4, 8.7 Hz, 1H), 7.00 (d, *J* = 8.4 Hz, 1H), 6.88 (d, *J* = 8.7 Hz, 1H), 4.81 (s, 2H), 3.85 (s, 3H), 3.80 (s, 3H), 3.70 (s, 6H); MS (ESI) *m/z*: 478 $[M+H]^+$.

(*E*)-N-(3,4-dimethoxyphenyl)-2-(4-(3-(3,4,5-trimethoxyphenyl)acryloyl)phenoxy) acetamide (54): It was synthesized from **27** (0.1 g, 0.44 mmol), K_2CO_3 (0.18 g, 1.33 mmol), and **6** (0.14 g, 0.44 mmol) as described in the general procedure C to yield **54** as a grey solid. Yield: 58%; TLC R_f = 0.45 (DCM:MeOH, 95:5); purity (HPLC): >99%; mp: 176-178 °C; ^{1}H-NMR (DMSO-d_6, 400 MHz) δ 10.03 (s, 1H), 8.19 (d, *J* = 8.6 Hz, 2H), 7.89 (d, *J* = 15.5 Hz, 1H), 7.66 (d, *J* = 15.5 Hz, 1H), 7.32 (d, *J* = 2.4 Hz, 1H), 7.22 (s, 2H), 7.16-7.14 (m, 3H), 6.90 (d, *J* = 8.8 Hz, 1H), 4.81 (s, 2H), 3.85 (s, 6H), 3.71-3.69 (m, 9H); MS (ESI) *m/z*: 508 $[M+H]^+$.

(*E*)-N-(3,4-dimethoxyphenyl)-2-(4-(3-(4-ethoxyphenyl)acryloyl)phenoxy)acetamide (55): It was synthesized from **27** (0.1 g, 0.44 mmol), K_2CO_3 (0.18 g, 1.33 mmol), and **20** (0.12 g, 0.44 mmol) as described in the general procedure C to yield **55** as a grey solid. Yield: 54%; TLC R_f = 0.51 (DCM:MeOH, 95:5); purity (HPLC): 98.46%; mp: 182-184 °C; ^{1}H-NMR (DMSO-d_6, 400 MHz) δ 10.02 (s, 1H), 8.16 (d, *J* = 8.3 Hz, 2H), 7.82-7.79 (m, 3H), 7.67 (d, *J* = 15.4 Hz, 1H), 7.32 (s, 1H), 7.17-7.12 (m, 3H), 6.99 (d, *J* = 8.3 Hz, 2H), 6.90 (d, *J* = 8.7 Hz, 1H), 4.80 (s, 2H), 4.08 (q, *J* = 7.0 Hz, 2H), 3.71 (s, 6H), 1.33 (t, *J* = 6.9 Hz, 3H); MS (ESI) *m/z*: 462 $[M+H]^+$.

(*E*)-2-(4-(3-(2-chlorophenyl)acryloyl)phenoxy)-N-(3,4-dimethoxyphenyl)acetamide (56): It was synthesized from **27** (0.1 g, 0.44 mmol), K_2CO_3 (0.18 g, 1.33 mmol), and **4** (0.11 g, 0.44 mmol) as described in the general procedure C to yield **56** as a grey solid. Yield: 60%; TLC R_f = 0.54 (DCM:MeOH, 95:5); purity (HPLC): >99%; mp: 198-200 °C; ^{1}H-NMR (DMSO-d_6, 400 MHz) δ 10.04 (s, 1H), 8.23-8.19 (m, 3H), 8.01 (s, 2H), 7.57-7.55 (m, 1H), 7.48-7.43 (m, 2H), 7.32 (d, *J* = 2.4 Hz, 1H), 7.17-7.15 (m, 3H), 6.90 (d, *J* = 8.7 Hz, 1H), 4.82 (s, 2H), 3.71 (s, 6H); MS (ESI) *m/z*: 452 $[M+H]^+$.

(*E*)-2-(4-(3-(4-chlorophenyl)acryloyl)phenoxy)-N-(3,4-dimethoxyphenyl)acetamide (57): It was synthesized from **27** (0.1 g, 0.44 mmol), K_2CO_3 (0.18 g, 1.33 mmol), and **16** (0.11 g, 0.44 mmol) as described in the general procedure C to yield **57** as a grey solid. Yield: 58%; TLC R_f = 0.55 (DCM:MeOH, 95:5); purity (HPLC): 98.78%; mp: 296-298 °C; ^{1}H-NMR (DMSO-d_6, 400 MHz) δ 10.18 (s, 1H), 8.20-8.18 (m, 2H), 8.00-7.91 (m, 3H), 7.69 (d, *J* = 15.5 Hz, 1H), 7.52-7.50 (m, 2H), 7.34 (d, *J* = 2.3 Hz, 1H), 7.18-7.14 (m, 3H), 6.89 (d, *J* = 8.7 Hz, 1H), 4.83 (s, 2H), 3.71 (s, 6H); MS (ESI) *m/z*: 452 $[M+H]^+$.

(*E*)-2-(4-(3-(2,6-difluorophenyl)acryloyl)phenoxy)-N-(3,4-dimethoxyphenyl)acetamide (58): It was synthesized from **27** (0.1 g, 0.44 mmol), K_2CO_3 (0.18 g, 1.33 mmol), and **7** (0.11 g,

0.44 mmol) as described in the general procedure C to yield **58** as a grey solid. Yield: 53%; TLC R_f = 0.58 (DCM:MeOH, 95:5); purity (HPLC): >99%; mp: 168-170 °C; ^{1}H-NMR (DMSO-d_6, 400 MHz) δ 10.02 (s, 1H), 8.08 (d, *J* = 7.8 Hz, 2H), 7.87 (d, *J* = 16.0 Hz, 1H), 7.67 (d, *J* = 15.6 Hz, 1H), 7.58-7.55 (m, 1H), 7.32-7.24 (m, 3H), 7.17-7.15 (m, 3H), 6.90 (d, *J* = 8.2 Hz, 1H), 4.81 (s, 2H), 3.71 (s, 6H); MS (ESI) *m/z*: 454 $[M+H]^+$.

(*E*)-N-(3,4-dimethoxyphenyl)-2-(4-(3-(furan-2-yl)acryloyl)phenoxy)acetamide (59): It was synthesized from **27** (0.1 g, 0.44 mmol), K_2CO_3 (0.18 g, 1.33 mmol), and **10** (0.09 g, 0.44 mmol) as described in the general procedure C to yield **59** as a grey solid. Yield: 56%; TLC R_f = 0.53 (DCM:MeOH, 95:5); purity (HPLC): >99%; mp: 260-262 °C; ^{1}H-NMR (DMSO-d_6, 400 MHz) δ 10.31 (s, 1H), 8.08 (d, *J* = 8.5 Hz, 2H), 7.90 (s, 1H), 7.54 (s, 2H), 7.36 (s, 1H), 7.19-7.08 (m, 4H), 6.89 (d, *J* = 8.6 Hz, 1H), 6.68 (s, 1H), 4.83 (s, 2H), 3.71 (s, 6H); MS (ESI) *m/z*: 408 $[M+H]^+$.

(*E*)-N-(3,4-dimethoxyphenyl)-2-(4-(3-(thiophen-2-yl)acryloyl)phenoxy)acetamide (60): It was synthesized from **27** (0.1 g, 0.44 mmol), K_2CO_3 (0.18 g, 1.33 mmol), and **3** (0.1 g, 0.44 mmol) as described in the general procedure C to yield **59** as a grey solid. Yield: 57%; TLC R_f = 0.52 (DCM:MeOH, 95:5); purity (HPLC): >99%; mp: 270-272 °C; ^{1}H-NMR (DMSO-d_6, 400 MHz)) δ 10.09 (s, 1H), 8.12 (d, *J* = 8.9 Hz, 2H), 7.87 (d, *J* = 15.3 Hz, 1H), 7.77 (d, *J* = 5.0 Hz, 1H), 7.67 (d, *J* = 3.5 Hz, 1H), 7.57 (d, *J* = 15.3 Hz, 1H), 7.33 (d, *J* = 2.4 Hz, 1H), 7.19-7.12 (m, 4H), 6.90 (d, *J* = 8.7 Hz, 1H), 4.81 (s, 2H), 3.71 (s, 6H); MS (ESI) *m/z*: 424 $[M+H]^+$.

(*E*)-N-(benzo[*d*][1,3]dioxol-5-ylmethyl)-2-(4-(3-(4-methoxyphenyl)acryloyl)phenoxy) acetamide (61): It was synthesized from **28** (0.1 g, 0.44 mmol), K_2CO_3 (0.18 g, 1.33 mmol), and **2** (0.11 g, 0.44 mmol) as described in the general procedure C to yield **61** as a light brown solid. Yield: 58%; TLC R_f = 0.53 (DCM:MeOH, 95:5); purity (HPLC): >99%; mp: 280-282 °C; ^{1}H-NMR (DMSO-d_6, 400 MHz) δ 8.70 (t, *J* = 6.1 Hz, 1H), 8.15 (d, *J* = 8.5 Hz, 2H), 7.85-7.79 (m, 3H), 7.68 (d, *J* = 15.5 Hz, 1H), 7.09 (d, *J* = 8.5 Hz, 2H), 7.01 (d, *J* = 8.4 Hz, 2H), 6.84-6.82 (m, 2H), 6.73 (d, *J* = 1.7, 7.9 Hz, 1H), 5.96 (s, 2H), 4.67 (s, 2H), 4.24 (d, *J* = 6.1 Hz, 2H), 3.81 (s, 3H).; MS (ESI) *m/z*: 446 $[M+H]^+$.

(*E*)-N-(benzo[*d*][1,3]dioxol-5-ylmethyl)-2-(4-(3-(3,4-dimethoxyphenyl)acryloyl)phenoxy) acetamide (62): It was synthesized from **28** (0.1 g, 0.44 mmol), K_2CO_3 (0.18 g, 1.33 mmol), and **1** (0.13 g, 0.44 mmol) as described in the general procedure C to yield **62** as a light brown

solid. Yield: 55%; TLC R_f = 0.51 (DCM:MeOH, 95:5); purity (HPLC): 98.56%; mp: 288-290 °C; ^{1}H-NMR (DMSO-d_6, 400 MHz) δ 8.67 (t, *J* = 6.2 Hz, 1H), 8.16 (d, *J* = 8.4 Hz, 2H), 7.83 (d, *J* = 15.5 Hz, 1H), 7.66 (d, *J* = 15.4 Hz, 1H), 7.53 (s, 1H), 7.37 (d, *J* = 8.2 Hz, 1H), 7.10 (d, *J* = 8.4 Hz, 2H), 7.01 (d, *J* = 8.3 Hz, 1H), 6.83 (d, *J* = 9.2 Hz, 2H), 6.73 (d, *J* = 8.0 Hz, 1H), 5.96 (s, 2H), 4.67 (s, 2H), 4.24 (d, *J* = 6.0 Hz, 2H), 3.85 (s, 3H), 3.80 (s, 3H); MS (ESI) *m/z*: 476 $[M+H]^+$.

(*E*)-N-(benzo[*d*][1,3]dioxol-5-ylmethyl)-2-(4-(3-(3,4,5-trimethoxyphenyl)acryloyl) phenoxy)acetamide (63): It was synthesized from **28** (0.1 g, 0.44 mmol), K_2CO_3 (0.18 g, 1.33 mmol), and **6** (0.14 g, 0.44 mmol) as described in the general procedure C to yield **63** as a light brown solid. Yield: 56%; TLC R_f = 0.49 (DCM:MeOH, 95:5); purity (HPLC): >99%; mp: >300 °C; ^{1}H-NMR (DMSO-d_6, 400 MHz) δ 8.68 (t, *J* = 6.1 Hz, 1H), 8.18 (d, *J* = 8.8 Hz, 2H), 7.89 (d, *J* = 15.5 Hz, 1H), 7.66 (d, *J* = 15.4 Hz, 1H), 7.22 (s, 2H), 7.11 (d, *J* = 8.8 Hz, 2H), 6.83-6.81 (m, 2H), 6.73 (d, *J* = 7.9 Hz, 1H), 5.96 (s, 2H), 4.68 (s, 2H), 4.24 (d, *J* = 6.1 Hz, 2H), 3.85 (s, 6H), 3.70 (s, 3H); MS (ESI) *m/z*: 506 $[M+H]^+$.

(*E*)-N-(benzo[*d*][1,3]dioxol-5-ylmethyl)-2-(4-(3-(4-ethoxyphenyl)acryloyl)phenoxy) acetamide (64): It was synthesized from **28** (0.1 g, 0.44 mmol), K_2CO_3 (0.18 g, 1.33 mmol), and **20** (0.12 g, 0.44 mmol) as described in the general procedure C to yield **64** as a light brown solid. Yield: 58%; TLC R_f = 0.54 (DCM:MeOH, 95:5); purity (HPLC): 97.61%; mp: 288-290 °C; ^{1}H-NMR (DMSO-d_6, 400 MHz) δ 8.67 (t, *J* = 6.1 Hz, 1H), 8.15 (d, *J* = 8.9 Hz, 2H), 7.84-7.79 (m, 3H), 7.67 (d, *J* = 15.5 Hz, 1H), 7.09 (d, *J* = 8.9 Hz, 2H), 6.99 (d, *J* = 8.8 Hz, 2H), 6.83-6.81 (m, 2H), 6.73 (d, *J* = 6.3 Hz, 1H), 5.96 (s, 2H), 4.67 (s, 2H), 4.24 (d, *J* = 6.1 Hz, 2H), 4.11-4.06 (m, 2H), 1.34 (t, *J* = 7.0 Hz, 3H); MS (ESI) *m/z*: 460 $[M+H]^+$.

(*E*)-N-(benzo[*d*][1,3]dioxol-5-ylmethyl)-2-(4-(3-(2,6-difluorophenyl)acryloyl)phenoxy) acetamide (65): It was synthesized from **28** (0.1 g, 0.44 mmol), K_2CO_3 (0.18 g, 1.33 mmol), and **7** (0.11 g, 0.44 mmol) as described in the general procedure C to yield **65** as a light brown solid. Yield: 59%; TLC R_f = 0.57 (DCM:MeOH, 95:5); purity (HPLC): >99%; mp: 290-292 °C; ^{1}H-NMR (DMSO-d_6, 400 MHz) δ 8.67 (t, *J* = 6.0 Hz, 1H), 8.06 (d, *J* = 8.5 Hz, 2H), 7.87 (d, *J* = 16.0 Hz, 1H), 7.67 (d, *J* = 16.0 Hz, 1H), 7.56 (p, *J* = 7.4 Hz, 1H), 7.26 (t, *J* = 8.8 Hz, 2H), 7.12 (d, *J* = 8.6 Hz, 2H), 6.83-6.80 (m, 2H), 6.72 (d, *J* = 8.0 Hz, 1H), 5.96 (s, 2H), 4.67 (s, 2H), 4.24 (d, *J* = 6.1 Hz, 2H); MS (ESI) *m/z*: 452 $[M+H]^+$.

4.3. Biological activity

4.3.1. In vitro *h*IMPDH2 enzyme inhibition assay [27,35]

The enzyme (*h*IMPDH2) was purchased from NovoCIB SAS (Lyon, France). A total of 37 molecules were screened at 10 µM concentration in the in vitro assay. The IC_{50} values were determined for molecules with >70 % inhibition at 10 µM. The assay was performed in in 96-well plates (Tarsons, 980040) (200 µL final volume) with a reaction buffer composed of 100 mM Tris–HCl (pH 8.6), 100 mM KCl and 5 mM DTT, 4% v/v DMSO plus or minus test compound and 0.15 mU of purified *h*IMPDH2 enzyme per well (from 1.5 mg/mL stock concentration). The final volume of the enzyme stock solution per well was 2 µL which was insignificant to cause any change in the final assay buffer composition. The reaction was initiated by the addition of (substrate buffer) 0.2 mM of IMP and 0.2 mM of NAD^+ and the assay was allowed to proceed at 37 °C for 30 min. The generated NADH was measured by reading the absorbance at 340 nm. At this wavelength, a background of <0.1 optical density (OD) was observed with negligible crosstalk between wells. Mycophenolic acid (10 µM) used as a positive control and DMSO as a vehicle control. For IC_{50} determination, a total of ten concentrations in triplicates were used (concentration ranged from 25 µM to 50 nM). Enzyme inhibition and IC_{50} were expressed in % inhibition and µM concentration, respectively.

4.3.2. Cell viability assay [46,48]

Cell lines such as MDA-MB-231 (breast adenocarcinoma), DU145 (prostate carcinoma), U87 MG (glioblastoma astrocytoma) and NIH-3T3 (mouse embryonic fibroblast) were purchased from National Centre for Cell Sciences (NCCS), Pune, India. Cytotoxic activity of the compounds (>80% *h*IMPDH2 inhibition at 10 µM) was evaluated using colorimetric MTT assay on above mentioned cell lines and MPA, doxorubicin and cisplatin as positive controls. Briefly, cells were grown in DMEM media supplemented with fetal bovine serum (FBS) 10% and penicillin-streptomycin (50 U/mL, 50 µg/mL) at 37 ºC, CO_2 (5%) and air (95%). Logarithmically growing cells were seeded in each of the 96-well plates at different concentration of test compounds ranging from 0.01 to 100 µM (seeding density: MDA-MB-231: 10,000 cells/well, DU145: 8,000 cells/well, U87 MG: 5,000 cells/well, NIH-3T3: 10,000 cells/well). After 24 hr of seeding, the cells were observed under microscope and treated with varying drug concentrations along with DMSO (vehicle control). Each dilution of the test compound was added in triplicate. Following 48 hr of incubation

with the compounds, cells were incubated with MTT reagent (5 mg/mL) for 4 hr, and then 100 µL of DMSO was added to dissolve formazan crystals. The absorbance was then measured at 540 nm and 630 nm (background scan) using EPOCH 2 Biotek microplate reader. The IC_{50} value (the compound concentration required to reduce the viability of the cells by 50% with respect to the control) for the tested compounds were calculated and expressed in µM using mean of triplicate readings.

4.4. Computational studies

Hardware and Software: All the molecular modelling studies described herein were performed on Dell Desktop (Intel® Core™ i3-7100T CPU @ 3.40 GHz, RAM 4 GB) running Windows 10 Pro Home Basic Operating System. Schrödinger Small-Molecule Drug Discovery Suite Release 2018-1 [49] and the products included therein were used for performing various molecular modelling operations described below.

4.4.1. *In silico* prediction of physicochemical property prediction

The calculated/predicted molecular/physicochemical properties of the synthesized compounds were generated using Canvas and QikProp modules of Schrödinger Small-Molecule Drug Discovery Suite. The compounds were first drawn in 2D, prepared using LigPrep module as per standard protocols. All the minimized structures were loaded into QikProp module and the physicochemical properties were predicted.

4.4.2. Molecular docking

To identify potential interactions of MPA (prototypical inhibitor) and the hits with *h*IMPDH2, molecular docking studies were performed using XP mode in the *GLIDE* module, with default settings. The X-ray structure of *h*IMPDH2 was retrieved from the protein data bank (PDB ID: 1JR1) and optimized by using OPLS2005 force field. All the hits were prepared and optimized using *LigPrep* module as implemented in Schrödinger Small-Molecule Drug Discovery Suite. Receptor grid was generated and the docking studies were performed according to the standard protocol. Individual docked poses were inspected manually to observe the binding interactions of ligands with *h*IMPDH2.

4.5. Determination of aqueous solubility and $logD_{7.4}$[50,51]

4.5.1. Standard calibration curve

Stock solutions ranging from 0.078 to 10 mM were prepared in DMSO. A mixture of sodium phosphate buffer (50 mM, pH 7.4) and acetonitrile in 1:1 ratio was used for further dilutions to get standard calibration curve having final concentration of 0.78, 1.56, 3.12, 6.25, 12.5, 25, 50 and 100 µM, respectively.

4.5.2. Solubility

Samples were prepared in sodium phosphate buffer (50 mM, pH 7.4) 990 µL and 10 µL from each stock solution and incubated at 37 °C for 2 hr in orbital shaker at 200 rpm. After incubation the samples were centrifuged at 4000 rpm for 20 min, supernatant was diluted with acetonitrile in 1:1 ratio and passed through syringe filter to ensure the removal of precipitate. The samples were then analysed by HPLC.

4.5.3. $logD_{7.4}$

In previously saturated solution of (1:1 ratio) 1-octanol and buffer (pH 7.4) 995 µL and 5 µL from each stock solution were added and incubated at 37 °C for 2 hr in orbital shaker at 200 rpm. Further 1-octanol and water layers were separated and analysed separately by HPLC and $logD_{7.4}$ calculated as the ratio of compound concentrations in 1-octanol to buffer phases.

4.5.4. HPLC analysis

HPLC analyses were performed using a Agilent1220 Infinity system equipped with a binary pump delivery system, a degasser, an autosampler, diode-array UV-VIS detector (DAD) and data elaboration were performed using Open Lab software (Agilent). All analysis was carried out at room temperature using the chromatographic conditions mentioned below. Column: C_{18} Kromasil® column (15 cm × 4.6 mm, 5 µm particle size, 100 Å pore size), mobile phase: Acetonitrile:Water (80:20, v/v)- isocratic, injection volume: 10 µL and flow rate: 1 mL/min.

Acknowledgements

CS and PK deeply acknowledge the help received from Dr. Kapil Juvale, Assistant Professor with SVKM's NMIMS, Shobhaben Pratapbhai Patel School of Pharmacy and Technology Management, Mumbai, India and Mr. Nitesh Sahu, PhD student in PK's group during *h*IMPDH2 inhibition studies and Department of Science and Technology (DST), Science and Engineering Research Board (SERB), Government of India for funding. The authors would

also like to thank Dr. Vikrant Bhor, Scientist D, National Institute for Research in Reproductive Health (NIRRH), Indian Council of Medical Research (ICMR) for hPBMC assay studies. The authors also thank Schrödinger LLC, NY, for providing one-month trial license of Schrödinger Small-Molecule Drug Discovery Suite to Dr. Mayur Yergeri, Professor at Shobhaben Pratapbhai Patel School of Pharmacy and Technology Management, Mumbai, India.

Conflicts of interest

The authors report no conflicts of interest. The authors alone are responsible for the content and writing of this article.

Funding

The authors acknowledge the financial support of their work by Young Scientist's Grant (No. SERB/LS-639/2013) awarded to PK from Science and Engineering Research Board (SERB), Department of Science and Technology (DST), Government of India.

References

[1] W. Qin, G. Huang, Z. Chen, Y. Zhang, Nanomaterials in targeting cancer stem cells for cancer therapy, Front. Pharmacol. 8 (2017) 1–15. doi:10.3389/fphar.2017.00001

[2] L. He, J. Gu, L.Y. Lim, Z.X. Yuan, J. Mo, Nanomedicine-mediated therapies to target breast cancer stem cells, Front. Pharmacol. 7 (2016) 1–13. doi:10.3389/fphar.2016.00313

[3] L. Zhang, R. Lv, X. Qu, X. Chen, H. Lu, Y. Wang, Aloesin Suppresses Cell Growth and Metastasis in Ovarian Cancer SKOV3 Cells through the Inhibition of the MAPK Signaling Pathway, Anal. Cell. Pathol. (Amst). 2017 (2017) 8158254. doi:10.1155/2017/8158254

[4] R. Petrelli, P. Vita, I. Torquati, K. Felczak, D.J. Wilson, P. Franchetti, L. Cappellacci, Novel inhibitors of inosine monophosphate dehydrogenase in patent literature of the last decade, Recent Pat. Anticancer Drug Discov. 8 (2013) 103–25. doi:10.2174/157489213805290600

[5] J.M. Reichert, J.B. Wenger, Development trends for new cancer therapeutics and vaccines, Drug Discov. Today. 13 (2008) 30–37. doi:10.1016/j.drudis.2007.09.003

[6] I. Ali, M.N. Lone, H.Y. Aboul-Enein, Imidazoles as potential anticancer agents, Med. Chem. Commun. 8 (2017) 1742–1773. doi:10.1039/C7MD00067G

[7] J. Iqbal, B.A. Abbasi, T. Mahmood, S. Kanwal, B. Ali, S.A. Shah, A.T. Khalil, Plant-derived anticancer agents: A green anticancer approach, Asian Pac. J. Trop. Biomed. 7 (2017) 1129–1150. doi: 10.1016/j.apjtb.2017.10.016

[8] A. Rana, J.M. Alex, M. Chauhan, G. Joshi, R. Kumar, A review on pharmacophoric designs of antiproliferative agents, Med. Chem. Res. 24 (2015) 903–920. doi:10.1007/s00044-014-1196-5

[9] K. Saleem, W. A. Wani, A. Haque, M.N. Lone, M. Hsieh, M.A. Jairajpuri, I. Ali, Synthesis , DNA binding , hemolysis assays and anticancer studies of copper (II), nickel (II) and iron (III) complexes of a pyrazoline-based ligand, Future Med. Chem. 5 (2013) 135–146. doi:10.4155/fmc.12.201

[10] a. C.P. Shah, P.S. Kharkar, Inosine 5′-monophosphate dehydrogenase inhibitors as antimicrobial agents: recent progress and future perspectives, Future Med. Chem. 7 (2015) 1415–1429. doi:10.4155/fmc.15.72; b. N.U. Sahu, V. Singh, D.M. Ferraris, M. Rizzi, P.S. Kharkar, Hit discovery of Mycobacterium tuberculosis inosine 5'-monophosphate dehydrogenase, GuaB2 inhibitors, Bioorganic Med. Chem. Lett. 28 (2018) 1714-1718. doi: 10.1016/j.bmcl.2018.04.045

[11] R.C. Jackson, G. Weber, H.P. Morris, IMP dehydrogenase, an enzyme linked with proliferation and malignancy, Nature. 256 (1975) 331–333. doi:10.1038/256331a0

[12] L. Hedstrom, IMP Dehydrogenase : Structure , Mechanism , and Inhibition, Chem. Rev. 109 (2009) 2903–2928. doi: 10.1021/cr900021w

[13] H.N. Jayaram, R.L. Dion, R.I. Glazer, D.G. Johns, R.K. Robins, P.C. Srivastava, D.A. Cooney, Initial studies on the mechanism of action of a new oncolytic thiazole nucleoside, 2-beta-D-ribofuranosylthiazole-4-carboxamide (NSC 286193), Biochem. Pharmacol. 31 (1982) 2371–2380. doi:10.1016/0006-2952(82)90532-9

[14] L. Manzoli, A.M. Billi, R.S. Gilmour, A.M. Marteili, A. Matteucci, S. Rubbini, G. Weber, L. Cocco, Phosphoinositide Signaling in Nuclei of Friend Cells: Tiazofurin Down-Regulates Phospholipase C β1, Cancer Res. 55 (1995) 2978–2980.

[15] R.A. Mandanas, D.S. Leibowitz, K. Gharehbaghi, T. Tauchi, G.S. Burgess, K. Miyazawa, H.N. Jayaram, H.S. Boswell, Role of p21 RAS in p210 *bcr-abl* transformation of murine myeloid cells, Blood. 82 (1993) 1838–1847.

[16] S.M. Kharbanda, M.L. Sherman, D.W. Kufe, Effects of tiazofurin on guanine

nucleotide binding regulatory proteins in HL-60 cells, Blood. 75 (1990) 583–588.

[17] M. Vitale, L. Zamai, E. Falcieri, G. Zauli, P. Gobbi, S. Santi, C. Cinti, G. Weber, IMP dehydrogenase inhibitor, tiazofurin, induces apoptosis in K562 human erythroleukemia cells, Commun. Clin. Cytom. 30 (1997) 61–66.

[18] H.R. Kim, J.S. Roe, J.E. Lee, I.Y. Hwang, E.J. Cho, H.D. Youn, A p53-inducible microRNA-34a downregulates Ras signaling by targeting IMPDH, Biochem. Biophys. Res. Commun. 418 (2012) 682–688. doi:10.1016/j.bbrc.2012.01.077

[19] E. Messina, P. Gazzaniga, V. Micheli, M.R. Guaglianone, S. Barbato, S. Morrone, L. Frati, A.M. Aglianó, A. Giacomello, Guanine nucleotide depletion triggers cell cycle arrest and apoptosis in human neuroblastoma cell lines, Int. J. Cancer. 108 (2004) 812–817. doi:10.1002/ijc.1164

[20] Y. Konno, Y. Natsumedasq, M. Nagai, Y. Yamaji, S. Ohnoq, G. Weber, Expression of Human IMP Dehydrogenase Types I and I1 in Escherichia coli and Distribution in Human Normal Lymphocytes and Leukemic Cell Lines , J. Biol. Chem. 266 (1991) 506–509.

[21] E. Olah, S. Kokeny, J. Papp, A. Bozsi, M. Keszei, Modulation of cancer pathways by inhibitors of guanylate metabolism, Adv. Enzyme Regul. 46 (2006) 176–190. doi:10.1016/j.advenzreg.2006.01.002

[22] R. Bentley, Mycophenolic acid: A one hundred year odyssey from antibiotic to immunosuppressant, Chem. Rev. 100 (2000) 3801–3825. doi:10.1021/cr990097b

[23] S.R. Knight, P.J. Morris, Does the evidence support the use of mycophenolate mofetil therapeutic drug monitoring in clinical practice? A systematic review, Transplantation. 85 (2008) 1675–1685. doi:10.1097/TP.0b013e3181744199

[24] V. Nair, Q. Shu, Inosine monophosphate dehydrogenase as a probe in antiviral drug discovery, Antivir. Chem. Chemother. 18 (2007) 245–258. doi:10.1177/095632020701800501

[25] Q. Shu, V. Nair, Inosine monophosphate dehydrogenase (IMPDH) as a target in drug discovery, Med. Res. Rev. 28 (2008) 219–232. doi:10.1002/med.20104

[26] G. Cholewinski, D. Iwaszkiewicz-Grzes, P. Trzonkowski, K. Dzierzbicka, Synthesis and biological activity of ester derivatives of mycophenolic acid and acridines/acridones as potential immunosuppressive agents, J. Enzyme Inhib. Med. Chem. 31 (2016) 974–982. doi:10.3109/14756366.2015.1077821

[27] T. Dunkern, S. Chavan, D. Bankar, A. Patil, P. Kulkarni, P.S. Kharkar, A. Prabhu, H.

Goebel, E. Rolser, W. Burckhard-Boer, P. Arumugam, M.T. Makhija, Design, synthesis and biological evaluation of novel inosine 5′-monophosphate dehydrogenase (IMPDH) inhibitors, J. Enzyme Inhib. Med. Chem. 29 (2014) 408–419. doi:10.3109/14756366.2013.793184

[28] T. Dunkern, A. Prabhu, P.S. Kharkar, H. Goebel, E. Rolser, W. Burckhard-Boer, P. Arumugam, M.T. Makhija, Virtual and experimental high-throughput screening (HTS) in search of novel inosine 5′-monophosphate dehydrogenase II (IMPDH II) inhibitors, J. Comput. Aided. Mol. Des. 26 (2012) 1277–92. doi:10.1007/s10822-012-9615-5

[29] G. Cholewiński, D. Iwaszkiewicz-Grześ, M. Prejs, A. Głowacka, K. Dzierzbicka, Synthesis of the inosine 5′-monophosphate dehydrogenase (IMPDH) inhibitors, J. Enzyme Inhib. Med. Chem. 30 (2015) 550–563. doi:10.3109/14756366.2014.951349

[30] J.J. Gu, L. Santiago, B.S. Mitchell, Synergy between imatinib and mycophenolic acid in inducing apoptosos in cell lines expressing Bcr-Abl, Blood. 105 (2005) 3270–3277. doi:10.1182/blood-2004-10-3864

[31] D.F. Jones, S.D. Mills, Preparation and Antitumor Properties of Analogs and Derivatives of Mycophenolic Acid, J. Med. Chem. 14 (1971) 305–311. doi:10.1021/jm00286a009

[32] S. Suzui, T. Sakae, M. Takashi, Antitumor activity of derivatives of mycophenolic acid, J. Antibiot. 29 (1976) 275-285.

[33] M. Malachowska-Ugarte, G. Cholewinski, K. Dzierzbicka, P. Trzonkowski, Synthesis and biological activity of novel mycophenolic acid conjugates containing nitro-acridine/acridone derivatives, Eur. J. Med. Chem. 54 (2012) 197–201. doi:10.1016/j.ejmech.2012.04.040

[34] D. Iwaszkiewicz-Grzes, G. Cholewinski, A. Kot-Wasik, P. Trzonkowski, K. Dzierzbicka, Synthesis and biological activity of mycophenolic acid-amino acid derivatives, Eur. J. Med. Chem. 69 (2013) 863–871. doi:10.1016/j.ejmech.2013.09.026

[35] C.P. Shah, P.S. Kharkar, Newer human inosine 5′-monophosphate dehydrogenase 2 (*h*IMPDH2) inhibitors as potential anticancer agents, J. Enzyme Inhib. Med. Chem. 33 (2018) 972-977. doi:10.1080/14756366.2018.1474211

[36] S. Domhan, S. Muschal, C. Schwager, C. Morath, U. Wirkner, W. Ansorge, C. Maercker, M. Zeier, P.E. Huber, A. Abdollahi, Molecular mechanisms of the antiangiogenic and antitumor effects of mycophenolic acid, Mol. Cancer Ther. 7 (2008) 1656–1668. doi:10.1158/1535-7163.MCT-08-0193

[37] H.H. Gu, E.J. Iwanowicz, J. Guo, S.H. Watterson, Z. Shen, W.J. Pitts, T.M. Dhar, C.A. Fleener, K. Rouleau, N.Z. Sherbina, M. Witmer, Novel diamide-based inhibitors of IMPDH, Bioorganic Med. Chem. Lett. 12 (2002) 1323–1326. doi:10.1016/S0960-894X(02)00132-4

[38] W.J. Pitts, J. Guo, T.M. Dhar, Z. Shen, H.H. Gu, S.H. Watterson, M.S. Bednarz, B.C. Chen, J.C. Barrish, D. Bassolino, D. Cheney, Rapid synthesis of triazine inhibitors of inosine monophosphate dehydrogenase, Bioorganic Med. Chem. Lett. 12 (2002) 2137–2140. doi:10.1016/S0960-894X(02)00351-7

[39] T.G. Murali Dhar, C. Liu, W.J. Pitts, J. Guo, S.H. Watterson, H. Gu, C.A. Fleener, K. Rouleau, N.Z. Sherbina, J.C. Barrish, D. Hollenbaugh, E.J. Iwanowicz, A survey of cyclic replacements for the central diamide moiety of inhibitors of inosine monophosphate dehydrogenase, Bioorganic Med. Chem. Lett. 12 (2002) 3125–3128. doi:10.1016/S0960-894X(02)00641-8

[40] T.G. Murali Dhar, Z. Shen, C.A. Fleener, K.A. Rouleau, J.C. Barrish, D.L. Hollenbaugh, E.J. Iwanowicz, The TosMIC approach to 3-(oxazol-5-yl) indoles: Application to the synthesis of indole-based IMPDH inhibitors, Bioorganic Med. Chem. Lett. 12 (2002) 3305–3308. doi:10.1016/S0960-894X(02)00748-5

[41] E.J. Iwanowicz, S.H. Watterson, C. Liu, H.H. Gu, T. Mitt, K. Leftheris, J.C. Barrish, C.A. Fleener, K. Rouleau, N.Z. Sherbina, D.L. Hollenbaugh, Novel guanidine-based inhibitors of inosine monophosphate dehydrogenase, Bioorganic Med. Chem. Lett. 12 (2002) 2059–2063. doi:10.1016/S0960-894X(03)00600-5

[42] S.H. Watterson, M. Carlsen, T.G. Murali Dhar, Z. Shen, W.J. Pitts, J. Guo, H.H. Gu, D. Norris, J. Chorba, P. Chen, D. Cheney, M. Witmer, C. A. Fleener, K. Rouleau, R. Townsend, D.L. Hollenbaugh, E.J. Iwanowicz, Novel inhibitors of IMPDH:a highly potent and selective quinolone-based series, Bioorganic Med. Chem. Lett. 13 (2003) 543–546. doi:10.1016/S0960-894X(02)00944-7

[43] N. Yang, Q.H. Wang, W.Q. Wang, J. Wang, F. Li, S.P. Tan, M.S. Cheng, The design, synthesis and in vitro immunosuppressive evaluation of novel isobenzofuran derivatives, Bioorganic Med. Chem. Lett. 22 (2012) 53–56. doi:10.1016/j.bmcl.2011.11.078

[44] M.D. Sintchak, E. Nimmesgern, The structure of inosine 5′-monophosphate dehydrogenase and the design of novel inhibitors, Immunopharmacology. 47 (2000) 163-184. doi:10.1016/S0162-3109(00)00193-4

[45] N. Yang, J. Wang, J. Li, Q.H. Wang, Y. Wang, M.S. Cheng, A three-dimensional pharmacophore model for IMPDH inhibitors, Chem. Biol. Drug Des. 78 (2011) 175–182. doi:10.1111/j.1747-0285.2011.01128.x

[46] K. Juvale, K. Stefan, M. Wiese, Synthesis and biological evaluation of flavones and benzoflavones as inhibitors of BCRP / ABCG2, Eur. J. Med. Chem. 67 (2013) 115–126. doi:10.1016/j.ejmech.2013.06.035

[47] K. Pissinate, D.C. Rostirolla, L.M. Pinherio, P. Suryadevara, P. Yogeeswari, D. Sriram, L.A. Basso, P. Machado, D.S. Santos, Synthesis and Evaluation of Thiazolyl-1H-benzo[*d*] imidazole inhibitors of Mycobacterium tuberculosis inosine monophosphate dehydrogenase, J. Braz. Chem. Soc. 26 (2015) 1357–1366. doi:10.5935/0103-5053.20150104

[48] G. Turan-Zitouni, M.D. Altintop, A. Özdemir, Z.A. Kaplancikli, G.A. Ciftci, H.E. Temel, Synthesis and evaluation of bis-thiazole derivatives as new anticancer agents, Eur. J. Med. Chem. 107 (2016) 288–294. doi:10.1016/j.ejmech.2015.11.002

[49] Schrödinger Small-Molecule Drug Discovery Suite Release 2018-1 is available from Schrödinger, LLC, New York, NY. (2018); Canvas, Schrödinger, LLC, New York, NY (2018); QikProp, Schrödinger, LLC, New York, NY (2018).

[50] D. Singh, Defining desirable natural product derived anticancer drug space: optimization of molecular physicochemical properties and ADMET attributes. ADMET and DMPK. 4 (2016) 98-113. doi: 10.5599/admet.4.2.291

[51] E. Rutkowska, K, Pajak, K, Jóźwiak, Lipophilicity--methods of determination and its role in medicinal chemistry. Acta Pol. Pharm. 70 (2013) 3-18.

Highlights

- Three novel series A, B and C were investigated for *h*IMPDH2 inhibition
- Series A exhibited potent in vitro *h*IMPDH2 inhibition
- All compounds exhibited better cellular potency and less toxicity against normal cells than MPA
- The hit molecules may potentially serve as leads for further studies